E&G Quaternary Sci. J., 75, 107–129, 2026
https://doi.org/10.5194/egqsj-75-107-2026
© Author(s) 2026. This work is distributed under
the Creative Commons Attribution 4.0 License.

Open Access E&G Quaternary Science Journal

Research article

Postglacial water level changes of a drowned lake and river system in northeastern Mecklenburg Bay, southern Baltic Sea

Julian Granzow, Franz Tauber, Helge W. Arz, Jacob Geersen, and Peter Feldens

Leibniz Institute for Baltic Sea Research Warnemünde, 18119 Warnemünde, Rostock, Germany

Correspondence: Peter Feldens (peter.feldens@io-warnemuende.de)

Relevant dates: Received: 19 February 2025 – Revised: 19 May 2026 – Accepted: 21 May 2026 – Published: 12 June 2026

How to cite: Granzow, J., Tauber, F., Arz, H. W., Geersen, J., and Feldens, P.: Postglacial water level changes of a drowned lake and river system in northeastern Mecklenburg Bay, southern Baltic Sea, E&G Quaternary Sci. J., 75, 107–129, https://doi.org/10.5194/egqsj-75-107-2026, 2026.

Abstract: The postglacial geological evolution of the southwestern Baltic Sea is marked by dynamic water level developments, accompanied by pronounced coastline displacements and associated changes in coastal geomorphological features. This study describes preserved remnants of paleo-landscapes in northeastern Mecklenburg Bay, dating to the period from the Baltic Ice Lake to the regression following the Ancylus Lake stage. The Late Pleistocene to Early Holocene geologic development of the area is reconstructed based on multibeam echo sounder, sidescan-sonar, and sediment echo sounder data; sediment core analysis; and visual seafloor imagery. The spatial distribution of Baltic Ice Lake deposits suggests a coastline at depths of 20 m below present sea level at the northeastern margin of Mecklenburg Bay during the Baltic Ice Lake's initial transgressive phase. The deposits are truncated by a regional erosional unconformity associated with the final regression following the Baltic Ice Lake highstand that marks the onset of lowstand conditions in the study area. A developing terrestrial environment was subsequently flooded by the Ancylus Lake. The Ancylus Lake highstand is constrained by peat and fine-grained limnic deposits in water depths of 19 m below present sea level. The acoustic data reveal a lacustrine environment throughout the Ancylus Lake stage until at least 10.2 ka cal BP. The regression at the end of the Ancylus Lake period is preserved by a northward-draining channel system cutting into Ancylus Lake sediments. The geometry of these channels suggests a water level drop of 6–7 m in northeastern Mecklenburg Bay, supporting a minor Ancylus Lake regression west of the Darss Sill. The findings provide insights into the water level development of a key threshold area in the southwestern Baltic Sea and therefore contribute to the reconstruction of the postglacial evolution of the entire Baltic Sea.

Kurzfassung: Die postglaziale geologische Entwicklung der südwestlichen Ostsee ist durch Fluktuationen des Wasserstands gekennzeichnet, die mit ausgeprägten Küstenverschiebungen und damit verbundenen Veränderungen der geomorphologischen Merkmale des Küstenraums einhergehen. Diese Studie beschreibt Überreste von Paläolandschaften im Nordosten der Mecklenburger Bucht, die aus der Zeit vom Baltischen Eissee bis zur Regression nach dem Ancylus-See Stadium stammen. Die geologische Entwicklung des Gebiets wird anhand von Daten aus Fächerecholoten, Seitensichtsonaren und Sedimentecholoten, Sedimentkernanalysen und Videobildern des Meeresbodens rekonstruiert. Die räumliche Verteilung der Ablagerungen des Baltischen Eissees deutet auf eine Küstenlinie in einer Tiefe

von 20 m unter dem heutigen Meeresspiegel am nordöstlichen Rand der Mecklenburgischen Bucht während der anfänglichen Transgressionsphase des Baltischen Eissees hin. Die Ablagerungen werden durch eine regionale erosive Diskordanz abgeschnitten, die mit der abschließenden Regression nach dem Höchststand des Baltischen Eissees in Verbindung steht. Eine sich anschließend entwickelnde terrestrische Umgebung wurde vom Ancylus-See überflutet. Der höchste Wasserstand des Ancylus-Sees wird durch Torf und limnische Ablagerungen in Wassertiefen von 19 m unter dem heutigen Meeresspiegel angezeigt. Die akustischen Daten bilden eine lakustrine Umgebung während des gesamten Ancylus-See Stadiums bis mindestens 10,2 ka. kal. BP ab. Der Rückgang am Ende der Ancylus-See Phase ist durch ein nach Norden abfließendes System kleiner Flüsse erhalten geblieben, welche sich in die Sedimente des Ancylus-Sees eingegraben haben. Die Geometrie dieser Kanäle deutet auf einen Wasserstandsrückgang von 6–7 m im Nordosten der Mecklenburger Bucht hin, was eine Regression des Ancylus-Sees westlich der Darss-Schwelle stützt. Die Ergebnisse liefern Einblicke in die Wasserstandsentwicklung eines wichtigen Schwellenbereichs im Südwesten der Ostsee und tragen somit zur Rekonstruktion der postglazialen Entwicklung der gesamten Ostsee bei.

1 Introduction

The postglacial geological evolution of the Baltic Sea is characterized by a complex interplay between eustatic seal level rise, spatially variable isostatic uplift and subsidence, and ice sheet retreat (Björck, 1995; Harff et al., 2011; Lampe et al., 2011). Following the recession of the Scandinavian ice sheet in the southwestern Baltic from about 17 ka cal BP (Hughes et al., 2016), the Baltic Sea evolved through the stages of the glaciolacustrine Baltic Ice Lake (BIL), the glaciomarine Yoldia Sea (YS), the freshwater Ancylus Lake (AL), and the brackish Littorina Sea (LS) (Björck, 1995). The general timeline of relevant events is summarized in Table 1. The BIL and AL stages in particular were characterized by large and rapid coastline fluctuations (Mörner, 1979; Svensson, 1991; Gustafsson and Westman, 2002), with water level fluctuations of up to 25 m (Lampe, 2005). However, the geologic history of the individual basins, the positions of paleoshorelines, and their associated water levels are still not fully resolved today (Hoffmann et al., 2009). In addition to geological interest, a detailed reconstruction of past shorelines is highly relevant for archeological prospection as flooded former terrestrial areas may host sites of archeological relevance. High-resolution reconstructions of paleo-coastlines are particularly relevant from the Mesolithic period onwards (Hansson et al., 2018), corresponding to the period from the BIL to the AL. This period marks a time of significant human presence and mobility in the Baltic Sea region, which is related to the hunter–gatherer lifestyle. These societies constructed megastructures and temporary settlements in areas of the Baltic Sea basin that are presently up to 21 m b.s.l. (below present sea level) (Rosentau et al., 2017; Geersen et al., 2024).

The area of the Darss Sill (Fig. 1) is particularly relevant for understanding the geological history of the Baltic Sea. It is located directly at the isostatic zero line (Stattegger and Leszczyńska, 2023; Harff et al., 2017) that separates the rising and subsiding parts of the Baltic Sea. Previous studies have identified the Darss Sill as a potential southwestern boundary of the AL. After ca. 10.4 ka cal BP (Björck, 2008), this dammed lake experienced a gradual or sudden drop in its water level, totaling between 5 (Björck et al., 2008) and 20 m (Kolp, 1986). This was initially attributed to failure of the paleo-threshold located at the Darss Sill since reconstructions suggested that the Øresund (Fig. 1), which functioned as an outlet of the BIL, was uplifted due to isostatic movements, leaving the Darss Sill as the lowest, i.e., water-level-controlling, threshold (Björck and Digerfeldt, 1991). Accordingly, erosion of the Kadet Channel in the Darss Sill caused a catastrophic outburst of the AL (Kolp, 1986; Björck, 1995), lowering the lake level to global sea level in possibly only 2–3 years (Novak and Björck, 1998). The outflow would have formed the "Dana River", draining through Fehmarn Belt and Great Belt into the Kattegat, and corresponds to the onset of fluvial and lacustrine conditions in these areas (Stattegger and Leszczyńska, 2023; Bendixen et al., 2017). This theory was supported by findings of an anomalous non-cyclic fluvial event with gradually decreasing flow velocities of up to $8\,m\,s^{-1}$ in the southern Kattegat related to the AL regression (Novak and Björck, 1998), indications of fluvial conditions at the time of the AL highstand in the Great Belt (Wiberg-Larsen et al., 2001), and massive erosion of the Kadet Channel during the AL period (Lemke and Kuijpers, 1995). However, the hypothesis of the AL draining through the Kadet Channel was questioned later as new findings indicated an absence of erosional features in the Darss Sill area (Bennike and Jensen, 1998; Lemke et al., 1999) and a lack of prograding bedforms on the Darss Sill or in the adjacent basins (Jensen et al., 1999; Lemke et al., 2001). In addition, deep channels in Fehmarn Belt that were considered to be part of the proposed Dana River were found to be not formed or reactivated by the AL drainage. Feldens and Schwarzer (2012) and Bendixen et al. (2017) found no evidence for major erosion or delta deposits in southern Kattegat. To resolve

this contrasting evidence, Björck et al. (2008) proposed a "calm drainage" of the AL, where the gradient to sea level would initially be 10 m (over a long distance from the Ancylus Lake to the North Sea), allowing for a more gentle outflow. Fluvial erosion would account for about 5 m of drawdown, and the global eustatic sea level rise of 2 cm a^{-1} at that time (Lambeck and Chappell, 2001) would fill the remaining difference.

Nevertheless, a regression pathway through the Darss Sill would still require an incised channel through the threshold to match the reconstructed post-regression water level east of the Darss Sill. As no evidence of this has been found so far (Jensen et al., 1997) and because other possible outlets (e.g., Øresund or Lake Vänern) are ruled out by most studies (Björck, 1995), the question regarding the outlet of the AL is not finally resolved. Following the AL period, a remarkable feature of the Littorina Transgression is the 8.2 ka event, with a rapid increase in water level linked to the abrupt melting of glacial ice and subsequent freshwater input into the oceans (Stattegger and Leszczyńska, 2023). This transgression resulted in the flooding of coastal areas, including the Darss Sill, with a water level rise of 18 m between 8.57 and 8.0 ka (Stattegger and Leszczyńska, 2023).

Despite its significance, the Darss Sill has not been in the focus of research for the past 15 years and thus has never been investigated with modern, high-resolution acoustic methods. Here, we employ a high-resolution surface and subsurface dataset in combination with sediment core analysis to examine the postglacial water level development in this area. The main objectives of the study are to (i) discuss preserved remains of BIL, YS, and AL landscapes at the southern boundary of the Darss Sill towards Mecklenburg Bay and (ii) describe their implications for the water level at the BIL and AL highstand and regression.

2 Regional setting

The study area (Fig. 1) is located at the eastern margin of Mecklenburg Bay (southwestern Baltic Sea), east of the Paleo–Darss threshold in depths around 20 m b.s.l. The site is situated on the isostatic zero line (Stattegger and Leszczyńska, 2023; Harff et al., 2011). Located between the German peninsula Fischland–Darss–Zingst (to the south) and the Danish island Falster (to the north, Fig. 1), the Darss Sill separates the Arkona Basin in the east and Mecklenburg Bay in the west and is a bottleneck for water exchange in the Baltic Sea today. This section provides a brief overview of the literature on the development of the Baltic Sea in the Mecklenburg Bay–Darss Sill–Arkona Basin area from the time of the Baltic Ice Lake to the early Littorina Transgression, followed by a description of their previously reported deposits in the study area.

2.1 Summary of the regional development since the BIL

The BIL, a proglacial meltwater lake, formed in response to ice sheet retreat in the Baltic Sea area from around 17 ka cal BP (Hughes et al., 2016) onwards. Separated by an erosional unconformity, two major stratigraphic units of the BIL are recognized in most studies of the southern Baltic Sea, associated with two transgressional stages (Bennike and Jensen, 1998; Jensen et al., 1997). The initial BIL (BILi) reached its highstand at the end of the Allerød chronozone at ca. 12.9 ka cal BP (Table 1, Naughton et al., 2023). For the southwestern Arkona Basin, a maximum water level of 20 m b.s.l. was reported by Jensen et al. (1997) at this time. Assuming the Darss Sill was at a paleo-water depth of 23–24 m b.s.l. at the end of the last Glacial (Paleo–Darss threshold, Jensen et al., 1997), the BILi must have inundated the Darss Sill and was therefore at least temporarily connected to Mecklenburg Bay. Ice retreat from the Mt. Billingen area (Fig. 1) then caused a regression of the BILi, and the water level in Mecklenburg Bay decreased by about 4–5 m (Jensen et al., 1997; Bennike and Jensen, 1998). In contrast, water level drops of 5–10 (Björck, 1995) and 10–15 m (Svensson, 1991) have been reported in the central Baltic. This illustrates that the Darss Sill was an important barrier during the BIL phase, separating Mecklenburg Bay and the southwestern Arkona Basin below 24 m b.s.l. (Lemke et al., 2001). The resulting water level during the following BIL lowstand period was situated between 35 (Lemke, 1998), 40 (Jensen et al., 1997; Lampe, 2005), or even 50 m b.s.l. (Lemke et al., 2002a) in the Arkona Basin. Local isolated lakes developed in Mecklenburg Bay (Jensen et al., 1997) and the eastern Fehmarn Belt (Feldens and Schwarzer, 2012).

As a consequence of the ice re-advance in the Younger Dryas around 12.7 ka cal BP (Lohne et al., 2012), the passageway to the North Sea at Mt. Billingen was blocked again, and a new transgressional phase began (Björck and Digerfeldt, 1984). The final BIL (BILf) reached its maximum water level around 11.5 ka cal BP (Regnéll et al., 2025). Deposits of the BILf are widespread east of the Darss Sill (Jensen and Stecher, 1992; Bennike and Jensen, 1998; Lemke et al., 1998) and were also found in Mecklenburg Bay (Bennike and Jensen, 1998; Jensen et al., 1999; Heinrich et al., 2018). According to Bennike and Jensen (1998), the maximum water level during the BILf phase was 20 m b.s.l. in the Arkona Basin. Inundating the Darss Sill, the BILf reached a similar highstand in Mecklenburg Bay (Bennike and Jensen, 1998; Jensen et al., 1999), and, for the Darss Sill, a maximum water level of 17 m b.s.l. was reported (Lemke et al., 1994). Correlating these water level reconstructions is not trivial, however, as most studies did not consider neotectonic movements (Kaiser, 2001; Schwarzer et al., 2000). Attempts to reconstruct the isostatic components (Lampe et al., 2011; Uścinowicz, 2003) show that there were considerable movements up to 0.8 m ka^{-1}, even in the last 8 kyr cal BP and already close to the isostatic zero-line (Harff et al., 2017).

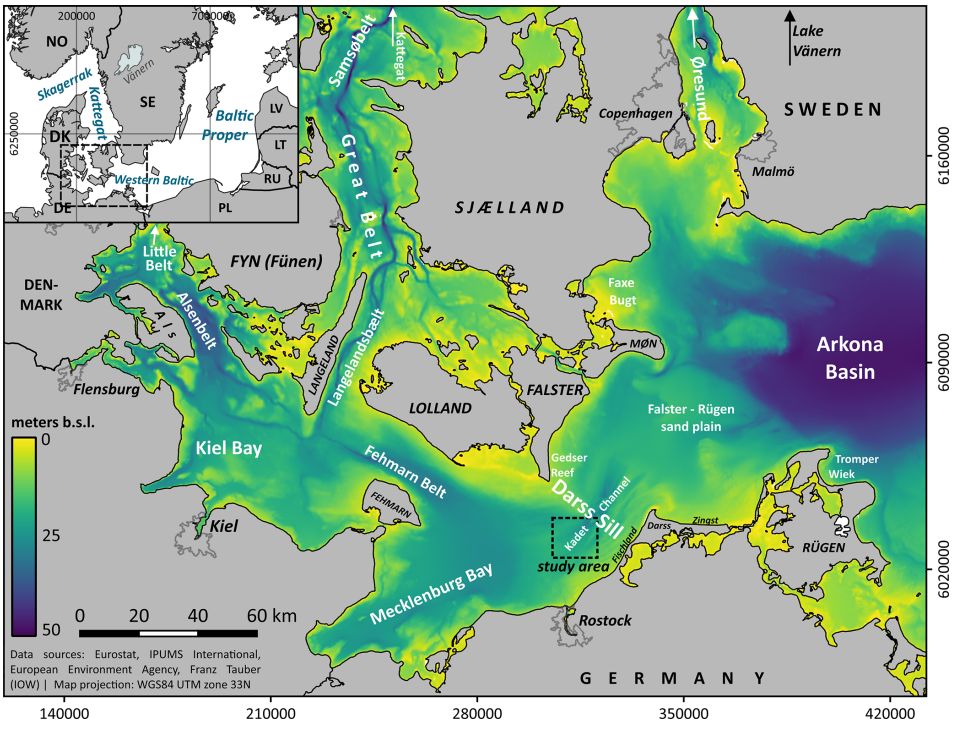


Figure 1. Location of the Darss Sill in the southwestern Baltic Sea, separating Mecklenburg Bay and the Arkona Basin. The location of the study area is indicated by the rectangle.

The final drainage of the BIL occurred when the ice retreated again from the Mt. Billingen area at the end of the Younger Dryas (Lampe, 2005). The consequence was another dramatic water level drop of 25–30 m (Björck, 1995; Lemke, 1998; Lambeck, 1999) over perhaps only 1–2 years (Johnson et al., 2013), corresponding to a sudden outflow of 7800 km^3 of freshwater into the North Sea and a reduction in the lake surface area by 18 % (Jakobsson et al., 2007). East of the Darss Sill, this resulted in a water level of 35 (Lemke, 1998), 40 (Björck, 1995; Jensen et al., 1997; Lampe, 2005), 45–50 (Lemke et al., 1998), or even 52 m b.s.l. (Uścinowicz, 2006), leading to fluvial and/or coastal lowstand conditions in the southwestern Arkona Basin (Lemke et al., 1998). West of the Darss Sill, the water level after the regression has been reconstructed to 30 m b.s.l. in Mecklenburg Bay (Kolp, 1965) and 35–38 m b.s.l. in the Fehmarn Belt (Jensen et al., 2005; Feldens and Schwarzer, 2012), leaving behind a shallow local waterbody (Lemke et al., 2002a). A water level drop of this magnitude led to a separation of the Arkona Basin and Mecklenburg Bay by the Darss Sill during the YS lowstand phase (Bennike and Jensen, 1998; Lemke et al., 1998, 2001), before the water level started to rise again, initiating the Ancylus Lake phase. Peat deposits have been described in Mecklenburg Bay at 26 m b.s.l. (Eronen et al., 1990) and have been dated to around 10.8 ka cal BP, corresponding to the onset of the AL transgression (Table 1).

The AL phase began when isostatic uplift in central Sweden once again isolated the Baltic proper from the world ocean (Lampe, 2005). This resulted in a synchronous transgression totaling 15–25 m in the southern Baltic Sea (Björck, 1995; Andrén et al., 2000) around 10.4 ka cal BP (Jensen et al., 1999). Analyses of shoreline displacement (Svensson, 1991) show that the AL was dammed above contemporaneous sea level. The most recent studies agree on a maximum water level between 18 and 20 m b.s.l. in Mecklenburg Bay (Jensen et al., 1997, 1999; Lemke, 1998; Bennike and Jensen, 1998; Kostecki et al., 2015; Lemke et al., 1997), the Darss Sill (Lemke et al., 1994; Bennike and Jensen, 1998), and the Arkona Basin (Bennike and Jensen, 1998; Jensen et al., 1999). Therefore, the AL inundated the Darss Sill threshold at least temporarily (Lemke et al., 2002a). On the Darss Sill, findings of lake marl have been linked to shallow lakes at the edge of the "main" AL (Lemke et al., 1994, 1997; Jensen et al., 1997; Bennike and Jensen, 1998; Bennike et al., 1998, 2004). After the AL regression, a lake remained in both the Arkona Basin and Mecklenburg Bay (Lemke et al., 2002a), while terrestrial conditions with isolated, local lakes prevailed on the Darss Sill (Bennike and Jensen, 1998; Bennike et al., 2004). The water level east of the Darss Sill was 32 m b.s.l. according to Kolp (1986) and Lemke et al. (1998, 2002a). The AL stage was followed by the Littorina Transgression, during which continued eustatic sea level rise and slowed isostatic rebound led to coastal flooding in the

Table 1. Description of events and dated materials. Conventional ages were converted to calendar years (IntCal20); already-calibrated ages were not further transformed. The calibrated result is rounded to 100 a for already-rounded uncalibrated ages or if the measurement accuracy is not specified. Calibrated ages are given as the median probability.

Event	^{14}C age (a BP)	Calibrated age (a BP)	Reference
Active ice leaves the SW Baltic Sea	–	ca. 17 000	Hughes et al. (2016)
Earliest phases of BIL, water level 25 m b.s.l.	13 500	ca. 16 300	Björck (1995), Lemke et al. (1998)
Water level of 30 m b.s.l. at Polish coast	13 000	15 600	Uścinowicz (2006)
Beginning of the BIL phase	12 600	ca. 15 000	Björck (1995)
End of rapid deglaciation in SW Baltic; Erosion in Øresund reaches the bedrock	12 000	13 900	Björck (1995)
Drainage of BILi, end of Allerød chronozone	11 200	12 900	Björck (1995), Naughton et al. (2023)
Readvancing Scandinavian Ice Sheet blocks, Mt. Billingen area, beginning of BILf transgression	–	12 800	Andrén et al. (2011)
Younger Dryas chronozone	–	12 710 ± 52 to 11 546 ± 59	Lohne et al. (2013)
BILf-max. transgression	–	11 570 ± 97	Regnéll et al. (2025)
YS phase	10 300–9500	11 500–10 800	Björck (1995), Regnéll et al. (2025)
Marine water entry in YS phase	9900	11 500	Björck (1995)
Peat deposits in Mecklenburg Bay and Tromper Wiek	ca. 9500	10 800	Eronen et al. (1990), Lemke et al. (2002b)
AL transgression	9500–9200	10 800–10 400	Jensen et al. (1999)
AL regression	9200–9000	10 400–10 200	Jensen et al. (1999)
Non-dammed AL	9000	10 200	Björck (1995)
Eustatic sea level rise reaches the lowered AL level	–	ca. 10 000	Björck et al. (2008)
Full marine conditions in southern Kattegat	8670 ± 90	9300	Bendixen et al. (2017)
Plant and animal macrofossils in lake marl in the SW Baltic	8500–7800	9500–8600	Bennike et al. (1998)
Rapid shore level rise from 14 to 4 m b.s.l. in the area of Fischland	–	9500–7500	Lampe et al. (2011)
Beginning of the Littorina Transgression in Mecklenburg Bay	–	8100	Bennike et al. (2021)

southern Baltic and the establishment of modern hydrological conditions.

2.2 Postglacial deposits

The succession of the respective Baltic Sea stages (Björck, 1995) led to a complex late-postglacial stratigraphy in the Darss Sill area, as detailed by Lemke et al. (1994, 1997), Lemke and Kuijpers (1995), and Jensen et al. (1997, 1999). The Quaternary deposits in the area locally exceed 40 m in thickness (Lemke et al., 1994), while the thickness of the late–postglacial sediments ranges from 6 m in the Kadet Channel (depth < 32 m) area to 18 m in the northeast (Lemke et al., 1994). However, in large parts between Falster and Fischland–Darss–Zingst, glacial till (Velgaster Staffel) crops out at the seafloor, often covered by a thin layer of lag sediment. Glaciolacustrine deposits of the BILi and BILf were identified in the eastern part of the Darss Sill and Gedser Reef up to 20 m b.s.l. (Lemke et al., 1994; Lemke and Kuijpers, 1995; Jensen et al., 1997; Bennike and Jensen, 1998), as well as in Mecklenburg Bay (Kostecki et al., 2015; Jensen et al., 1997; Heinrich et al., 2018). These deposits consist of organic-poor laminated silts and sands or annually varved clays in distal parts (Jensen and Stecher, 1992; Lemke et al., 1994; Jensen et al., 1997; Lemke et al., 1998; Andrén et al., 2002). In contrast, a more sandy and partly organic-rich facies developed in coastal and/or proximal locations such as the southern Darss Sill (Jensen et al., 1997). These deposits are commonly associated with the final phase of the BILf (Lemke et al., 1994, 2001; Jensen et al., 1997; Bennike and Jensen, 1998). The two BIL phases are usually separated by an erosional unconformity (Bennike and Jensen, 1998; Jensen et al., 1997, 1999; Lemke et al., 2002a; Bennike and Jensen, 1995, 2013).

Terrestrial deposits on the Darss Sill and adjacent basins developed in response to the lowstand conditions during the YS and subsequent AL stages (Bennike and Jensen, 1998; Feldens and Schwarzer, 2012; Hansson et al., 2018). In Mecklenburg Bay, peat, peat gyttja, and organic detritus were found to be related to a local lake and swamp environment and were dated to the onset of the YS lowstand period at around 11.5 ka cal BP (Eronen et al., 1990; Bennike and Jensen, 1998; Jensen et al., 1999; Kostecki et al., 2015). On the Darss Sill, fine-grained lake marl, lake chalk, calcareous gyttja with freshwater mollusks and plant remains, and peat deposits are widespread in water depths of < 19 m b.s.l. (Winn et al., 1982; Lemke and Kuijpers, 1995; Bennike and Jensen, 1998; Jensen et al., 1999; Tauber, 2012).

These sediments developed in local, isolated lakes during the AL and early LS stage as the Darss Sill was in a marginal and/or coastal position during that time. Peat accumulation was probably due to rising groundwater levels, associated with the AL transgression starting at 10.8 ka cal BP (Eronen et al., 1990; Lemke et al., 2002b). East of the Kadet Channel, Tauber (2011) described an ancient riverbed, represented by a strip of peat situated above tree stumps, dated to ca. 10.3–11.1 ka cal BP, i.e., spanning both YS and AL stages in time. It was hypothesized that the Kadet Channel is an older formation infilled with erodible sediment in YS times (Tauber, 2011). Similar remnants of a former fluvial environment spread over 7 km are also preserved north of the Zingst peninsula in water depths around 5–10 m b.s.l. (Tauber, 2011). LS deposits represent the youngest formations in shallow waters in the study area and have a fine to medium sand composition with marine shells, while silt deposits are found below 20 m water depth towards Mecklenburg Bay and the southwestern Arkona basin (Lemke et al., 1994, 2001; Lemke and Kuijpers, 1995; Bennike and Jensen, 1998). The thickness of LS deposits rarely exceeds 2–3 m (Lemke, 1998).

3 Methods

3.1 Acoustic data

Bathymetric grids with a resolution of 10 m were supplied by the German Federal Maritime Hydrographic Agency (BSH) for research purposes. Sidescan surveys of this area were conducted by the Leibniz-Institute for Baltic Sea Research Warnemünde (IOW) as part of the SINCOS (Sinking Coasts – Geosphere, Ecosphere and Anthroposphere of the Holocene Southern Baltic Sea) project in 2005 and the following years using an EG&G DF-1000 dual-frequency sidescan-sonar at 100 and 384 kHz. The Department of Hydrographic Surveying and Marine Geodesy at the BSH contributed raw sidescan-sonar data, recorded using an EdgeTech 4300 MPX multipulse system at 400 kHz during surveys in 2006 and 2007. Additional sidescan-sonar data were acquired during cruise EMB176 (13–21 February 2018) and EMB306 (22–30 November 2022) aboard RV *Elisabeth Mann Borgese*. These data were recorded using a Klein 4000 sidescan-sonar at 100 and 400 kHz frequencies. For the BSH data, backscatter mosaics with a resolution of 1 m were created using the 384 kHz channel, employing a custom processing script. In this study, higher backscatter intensities are displayed in darker colors. A multi-frequency mosaic was processed from the sidescan data acquired during the EMB176 cruise, following the method described in Tauber (2011), which accentuates sedimentological variations (Schulze et al., 2022). Coarser and acoustically harder materials, such as lag sediments, are generally depicted in red-brown colors, while sands predominantly appear in bluish hues.

Sediment echo sounder data were recorded between 2005 and 2022 on board *RV Elisabeth Mann Borgese* during various research cruises using the parametric Innomar Medium Sediment Echo Sounder with the low frequency set between 4 and 12 kHz. Profile lines were converted from the native .ses format to .sgy and imported into Kingdom Suite. A constant sound velocity of 1500 m s^{-1} was assumed for converting travel time into water depth in Fig. 3. Algorithms written in Visual C++ were applied to the data in .ses format to create the detailed channel insets shown in Fig. 5 and to locate cross-sections of the channels in ArcMap in the background of the sidescan-sonar mosaic for Fig. 4.

3.2 Sediment cores

Five sediment cores were collected from depths of 19–22 m b.s.l. using a 1 t gravity corer with a 4 m long steel tube during the research cruise EMB176 (13–21 August 2018) and a 4 m long vibro-corer during cruise EMB382 (15–17 July 2025). Core penetration depth ranged from 12 to 384 cm. In the laboratory, a visual description to identify lithological units (LUs) was done, considering color (Munsell Soil Color Chart; Munsell, 2000), organic matter content (including macroscopic organic remains such as plant roots, wood, or shell fragments), texture, and structural features. Samples for grain size analysis were extracted approximately every 5–10 cm, with additional samples taken from areas displaying visible irregularities such as lens structures. Before the measurement, each sample retrieved during EMB176 was treated with 10 mL of 10 % HCl for 4 h to remove carbonates, 10 mL of 30 % H_2O_2 for 24 h to remove organic matter, and 3 mL of sodium pyrophosphate as a dispersing agent. Samples retrieved during EMB382 were not pre-treated due to a change in lab routines; however, test analyses indicate no major differences in the results. The grain size distribution was determined by a laser diffraction particle size analyzer (Malvern Panalytical Mastersizer 3000) 12 times for each sample. The results were averaged and then analyzed in GRADISTAT v.9.1 (Blott and Pye, 2001) using the Folk and Ward method. For radiocarbon dating, peat, wood and plant roots were extracted from the cores and analyzed by Beta Analytics (Miami) using accelerator mass spectrometry (AMS). The conventional ages were calibrated with IntCal20 to calender years (Reimer et al., 2020). In this study, ages are reported as ka cal BP with a 95 % (2σ) confidence interval. By convention, the term BP refers to dates before the year 1950 (Godwin, 1962).

3.3 Seafloor photography

Visual images of the seafloor were captured using a Hydrovision Hyball remotely operated vehicle (ROV) during cruise 40/05/19 on RV *Prof. Albrecht Penck*. Video data were collected between 7 and 8 October 2005 (SINCOS station 316110 on 8 October 2005, 06:45–07:20 UTC; SINCOS sta-

tion 316060 on 7 October 2005, 08:10–09:05 UTC; SINCOS station 316090 on 7 October 2005, 15:10–15:55 UTC) from the anchoring vessel, with 80–100 m of cable released during the ROV operation.

4 Results

4.1 Acoustic data

4.1.1 Surface

The bathymetric and backscatter data (Fig. 2a) show the transition from the easternmost part of Mecklenburg Bay to the Darss Sill. Southwest of the narrow entrance of the Kadet Channel, the water depth is 23–24 m b.s.l. The seafloor then rises gently towards the west and gradually flattens out at ca. 18 m b.s.l., with a uniform and smooth morphology. In contrast, the area around 19–20 m b.s.l. south of station EMB176-45-1 is characterized by a more complex seabed morphology (Fig. 2a). Here, several roughly north–south-trending dunes with a meandering crest line are observed. These dunes have a length of up to 2 km and rise approximately 0.5–1 m above the surrounding seabed, reaching depths up to 18–21 m b.s.l., with the majority capped at 20 m b.s.l. The structures vanish in the west, where the water depth decreases to 18 m b.s.l. The dunes are barely noticeable in backscatter data and only show slightly higher backscatter intensities on their crests.

Farther south, the north–south dunes merge into an east–west-trending bathymetric high at depths around 18 m b.s.l. (along core 4775/13 (Bennike and Jensen, 1998), EMB176-47-1 and SINCOS station 316110; Fig. 2a). This structure represents a platform that rises ca. 1–1.5 m above the adjacent seabed and is composed of gyttja and peat sediment. In the backscatter data, the northern boundary of this platform can be recognized as a distinct linear feature. The platform was sampled by EMB176-47-1 and EMB382-5-1 in the west and EMB176-49-1 in the east. The structure extends for at least 3 km as an extensive, well-delineated feature. It is notably characterized by its low backscatter intensity and otherwise homogeneous appearance in both backscatter and bathymetric data (Fig. 2a, b).

South of the platform, the seafloor is characterized by a chaotic, unstructured morphology in water depths of ca. 18–19 m b.s.l. Backscatter and bathymetric data reveal the presence of both roughly circular depressions with diameters of 100–200 m and irregular elevations that rise ca. 0.4–1 m above the adjacent seafloor (Fig. 2a). These features occur in an area that extends > 10 km in east–west direction and 2–5 km in north–south direction. In the shallower (< 18 m b.s.l.) areas farther south, the morphology is homogeneous (Fig. 2a).

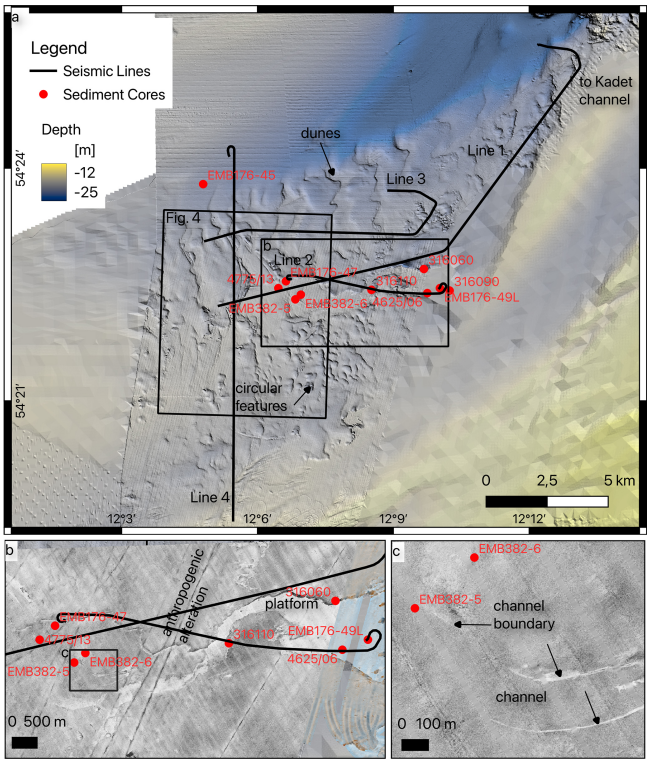


Figure 2. **(a)** Bathymetric features in the study area. The locations of sediment cores and SINCOS stations (this study), as well as core 4775/13 (Bennike and Jensen, 1998) and core 4625/06 (Lemke, 1998), are indicated by the red dots. **(b)** An extended platform composed of limnic deposits with low backscatter intensity in sidescan-sonar backscatter mosaics. **(c)** Adjacent to the platform, the boundaries of former channel systems can be recognized. Core EMB382-5-1 samples this channel system. In **(b)** and **(c)**, higher backscatter intensities are displayed in darker colors.

4.1.2 Subsurface

Seismic lines are shown in Fig. 3. This figure includes magnified examples of each seismic unit (SU) described here. SU 1 represents the limit of acoustic penetration and is not consistently identified across all seismic lines. Where discernible, its upper boundary is marked by a high-amplitude interface exhibiting a rough morphology that forms the base of acoustic penetration.

SU 2 is situated directly above SU 1 and recognized below 20 m b.s.l. It is distinguished from SU 1 by its faint, often bent and disrupted laminations. Meter-thick transparent segments are intermittently layered within the laminated sequences (best visible in the NE of Line 2 and the south of Line 4, Fig. 3).

SU 3 is divided into two subunits. SU 3a unconformably overlies SU 2 and is characterized by a predominantly chaotic internal structure to low-amplitude internal lamination. Nonetheless, it contains some internal, thick, high-amplitude layers. SU 3a is exposed at the base of video sta-

tion SINCOS 316060 (Fig. 8b), where it is truncated and under erosion. SU 3b is unconformably positioned over SU 2 or SU 1. SU 3b is observed below water depths of 20–21 m and is absent in shallower regions. It is defined by a dense array of high-amplitude reflectors that are internally more uniform and sub-parallel compared to SU 2. Unlike SU 2, SU 3b lacks thick transparent layers but features laminations with an apparent inclination in the northern part of the study area. SU 3b is best observed in the northern part of Line 4 (Fig. 3).

SU 4 is marked by a predominantly conformable but occasionally unconformable interface, marked by a high-amplitude reflector with the underlying SU 3a. SU 4 reaches depths not shallower than 19 m b.s.l., where it crops out at the seafloor and correlates with low-backscatter zones in sidescan-sonar imagery. It is divided into two subunits based on their different stratigraphic position, best observed in the southwestern part of Line 1 and the central part of Line 4 (Fig. 3). SU 4a is laterally truncated, indicative of erosion that has removed the majority of a former continuous surface (Line 1 in Fig. 3). Rough seafloor and circular features observed in bathymetric data (Fig. 2a) are created by these erosional activities. SU 4a correlates with small cliffs identified in bathymetric data and observed in underwater video footage (Figs. 3, 8). In contrast, SU 4b infills channels incised into SU 3a and 4a and partly SU 2, with inclined interbedded layers of varying amplitude, and it is observed in seismic lines recorded in water depths from 19 to 21 m b.s.l. Three continuous channel branches can be identified based on the backscatter and seismic data and are displayed in detail in Figs. 4 and 5. Of the three channel branches, the western channel is, on average, about 280 m wide (max. 330 m at its widest point), the middle channel is about 120 m (max. 180 m), and the eastern channel is about 120 m (max. 160 m). In some instances, erosion of adjacent sediments elevates the channel rims, which form distinct peaks on the seafloor (best observed in Profiles C1 and C3 in Fig. 5). The base of the channels is not always recognized, limited by the seismic signal's penetration depth. Where visible, the channels exhibit an incision depth of 6–7 m (Fig. 5). In particular, for the westernmost branch (A1 to A3 in Fig. 5), free gas obscures the maximum incision depth. Where the bottom of the channel is visible, the westernmost channel has an asymmetric bed shape (Profiles A1 to A3 in Fig. 5) with a steeper eastern side. The central and eastern branches show a symmetrical appearance of the channel bed.

SU 5a can be noted in water depths below 22 m b.s.l., where it unconformably overlies the basement (SU 3b or SU 2, best observed in the northern part of Line 4, Fig. 3). It exhibits a thickness of up to 2.5 m, decreasing from the west towards the narrow Kadet Channel across the Darss Sill. SU 5a appears to be homogeneous in the seismic data. SU 5b forms the current seafloor where present, creating an undulating surface as described in Sect. 4.1.1 (Line 3 in Fig. 3 and eastward end of profile B2 and C3 in Fig. 5), separated from a distinct high-amplitude reflector from the basement. These features are interpreted based on their internal structure and morphological characteristics as a series of elevated subaqueous dunes likely shaped by recent bottom currents and occur in water depths of 18–21 m b.s.l. (also see Fig. 2).

4.2 Sediment cores

4.2.1 Sediment core EMB176-45-1

Core EMB176-45-1 was retrieved from a water depth of 21.4 m north of the channel system described above (Fig. 4), penetrating SU 3b and 5. It contains 265 cm of sediment, divided into two lithological units (LUs, Fig. 6). LU 1 (0–28.5 cm) consists of poorly sorted, homogeneous fine sand with an average grain size of 93 µm. In its upper part (ca. 0–5 cm), the sediment has a darker color and contains poorly preserved shell fragments. The transition to LU 2 is marked by an erosional unconformity enriched with plant remains and humic particles. It is characterized by very poorly sorted, bimodally distributed grain sizes with high fine-sand (36 %), medium-sand (22 %), and coarse-silt (18 %) contents. In contrast, LU 2 (28.5–265 cm) features a grayish, stratified sediment with smaller average grain sizes. The sediment generally consists of poorly sorted, very fine skewed, mesokurtically–leptokurtically distributed coarse silt with average grain sizes ranging from 36 to 60 µm. Coarse layers of variable thickness occur irregularly throughout the unit. These layers are composed of well to moderately sorted, very leptokurtic, symmetrically distributed fine sand with average grain sizes of 92–127 µm. Below 215 cm, well-distinguishable coarse layers in wide alternation can be recognized. Between ca. 135–215 cm, a narrower alternating bedding of these layers can be observed. In the upper part of the unit (28.5–135 cm), the stratification is replaced gradually by a lens-like structure of coarse-grained deposits within finer sediment. Furthermore, the sediment contains poorly preserved plant remains, particularly humic particles. The latter occur preferably within the coarse-grained layers. Radiocarbon dating on a piece of wood reveals an age of 13 788–13 595 a cal BP and a δ^{13}C value of −29.0 ‰ at a core depth of 38–40 cm.

4.2.2 Sediment core EMB176-47-1

Core EMB176-47-1 (Fig. 6) recovered approx. 13 cm of sediment from a water depth of 19.5 m, adjacent to an incised channel and recovered the youngest preserved stratigraphy of SU 4a eroded by the channel system. The core is composed of two lithological units separated by an erosional unconformity. Poorly sorted fine to medium sand (average grain size 128 µm) with shell fragments comprises LU 1 (0–1.5 cm). Below the erosional unconformity, LU 2 (1.5–13 cm) is composed of black organic-rich sediment with micro- and macroscopic plant fragments. Radiocarbon dating on plant remains extracted from this section at 3–6 cm yielded an age of 10 765–10 578 a cal BP and a δ^{13}C value of −26.8 ‰ (Ta-

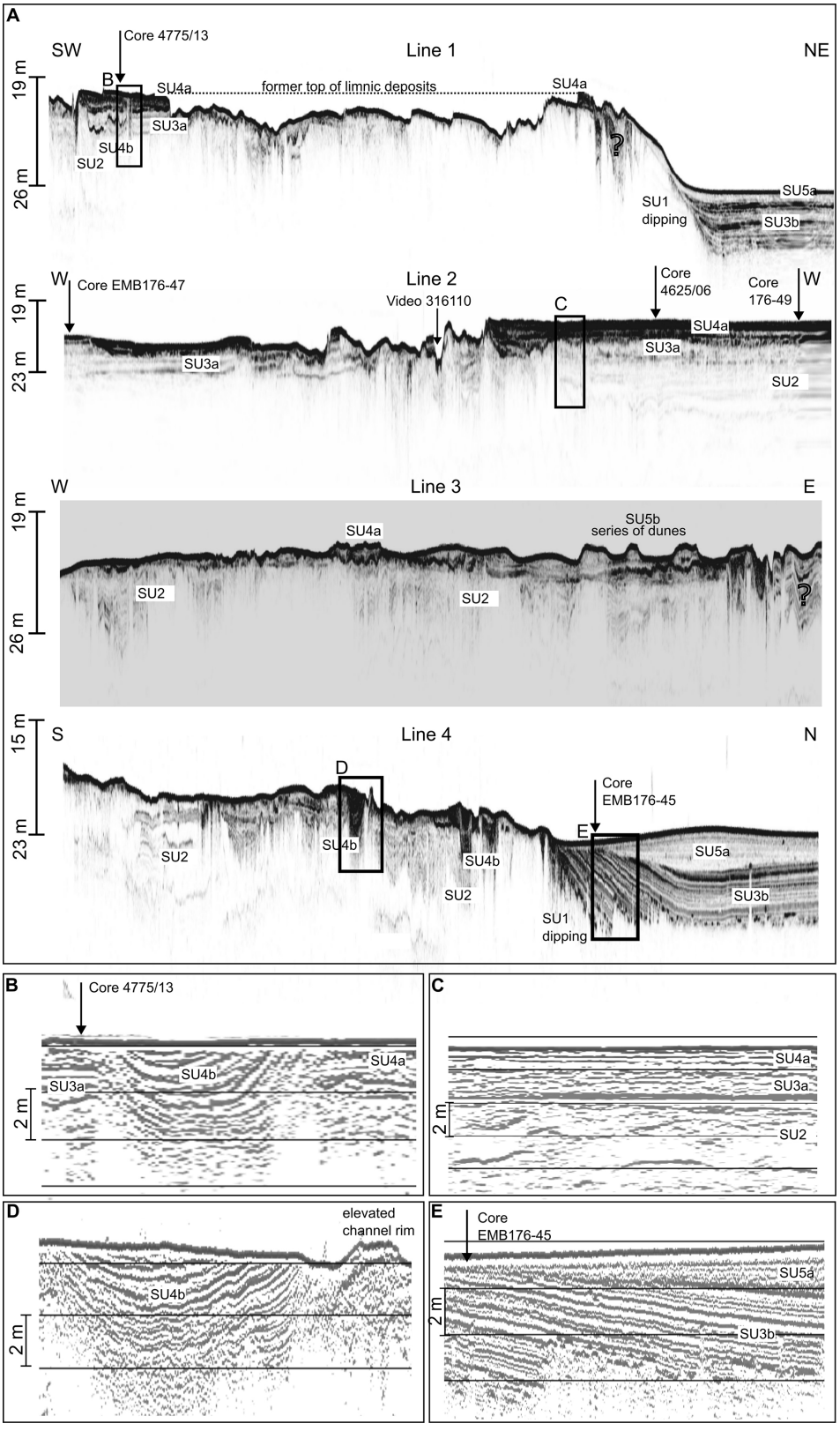


Figure 3. **(A)** Sediment echo sounder profiles, highlighting the described seismic units in the study area. The position of the seismic lines is given in Fig. 2. Two-way travel times were converted to depth using a sound velocity of 1500 m s^{-1}. **(B)–(E)** Insets of the profiles highlighting the texture of the seismic units (SU).

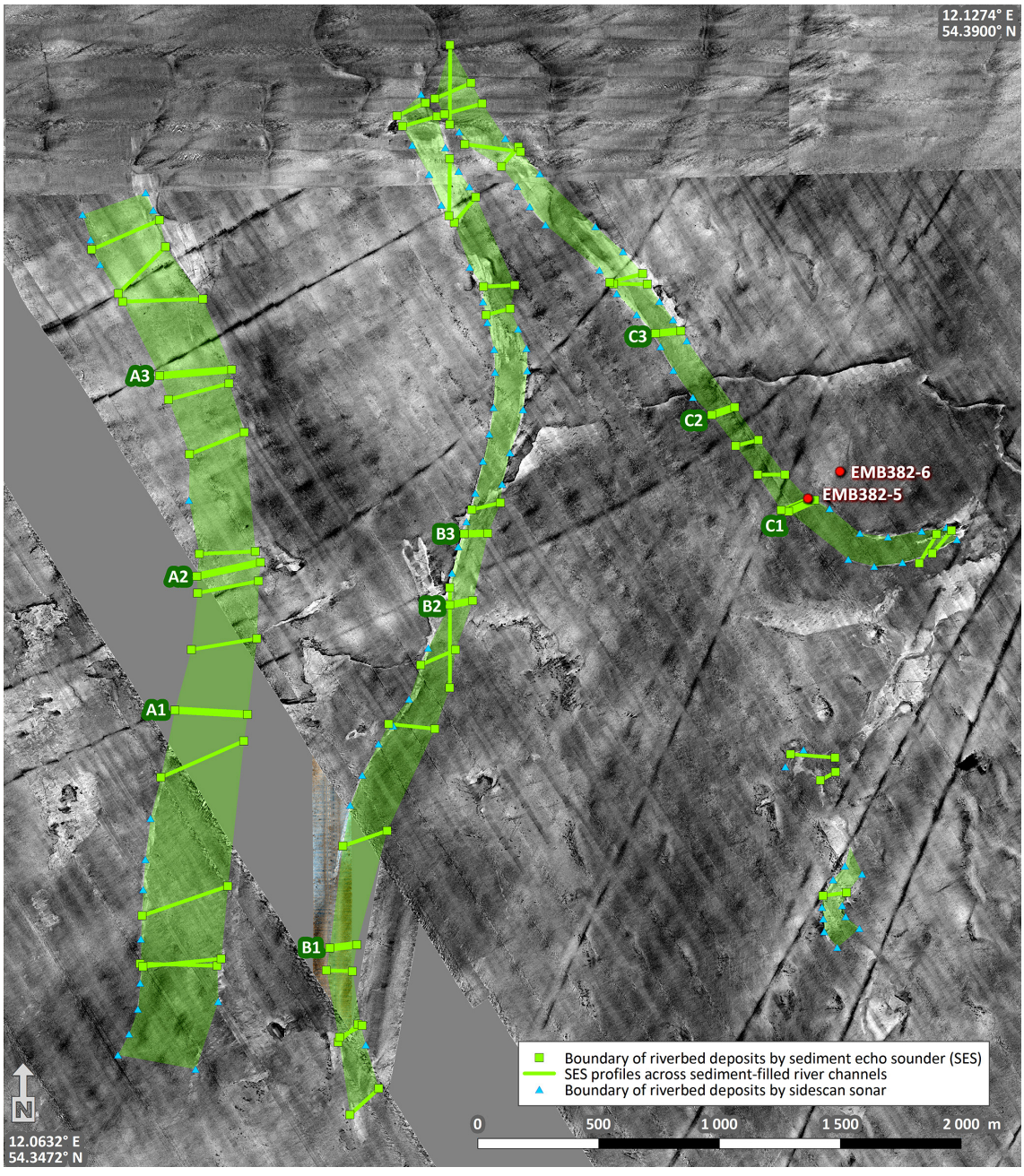


Figure 4. Cross-sections of the three identified branches of the channel system (SU 4c) as identified in seismic data, plotted in sidescan-sonar backscatter mosaics. Higher backscatter intensities are displayed in darker colors. For the location of the study site, refer to Fig. 2. Detailed seismic lines with incisions A1 to A3, B1 to B3, and C1 to C3 are displayed in Fig. 5.

ble 2). The average grain size is 22–32 µm with a poorly sorted distribution.

4.2.3 Sediment core EMB176-49-1

Core EMB176-49-1 sampled a low-backscatter platform (corresponding to SU 4a) observed in sidescan-sonar data and was retrieved from a water depth of 19.2 m. The core is 44 cm long (Fig. 6) and was divided into four lithological units. LU 1 (0–18 cm) consists of dark-gray sediment with little structure and is interspersed with fine plant remains (especially plant roots). Radiocarbon dating in 11–13 cm core depth on extracted plant material yielded an age of 10 242–10 185 a cal BP and a $\delta^{13}C$ value of −9.9 ‰ (Table 2), suggesting remains of aquatic plants and an overestimated age due to the hard-water effect. The main grain size fractions are medium and coarse silt (each up to about 40 %), result-

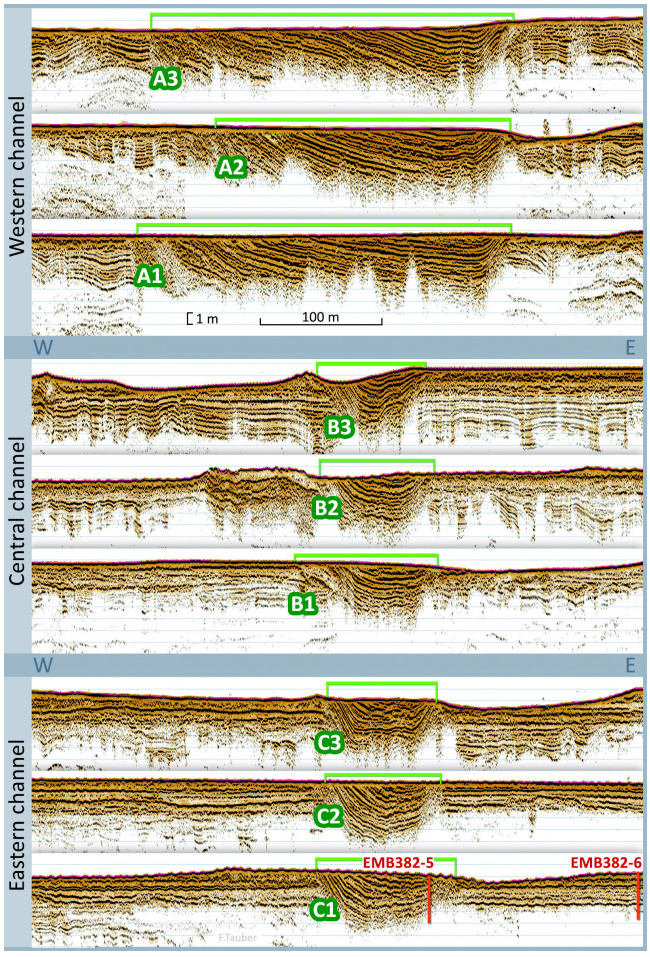


Figure 5. Cross-sections of the identified branches of the channel system (SU 4b). The lateral extent of the incisions is marked with green lines. The geographical positions of the channels are given in Fig. 4 as green lines.

ing in poor sorting. The average grain size increases from the unit's top (15 µm) to its base (23 µm). LU 2 (18–24.5 cm) is characterized by an irregularly structured sediment featuring diffuse fine-sandy, light-gray lens structures within silty sediment. The grain size distribution is bimodal, with peaks in the medium- to coarse-silt and fine-sand fractions. The average grain size is 32 µm. LU 3 (24.5–36 cm) has a similar color and grain size distribution to LU 1, with an average grain size of 17 µm. LU 4 (36–45 cm) contains a dark-gray sediment without macroscopically identifiable plant remains. The grain size distribution shows better sorting with about 40 % coarse silt and fine sand and an average grain size well above units 1 to 3 at about 50 µm.

4.2.4 Sediment core EMB382-5-1

Approximately 366 cm of sediment was recovered from the edge of the eastern channel of the paleo-river system at 19.0 m b.s.l. (Figs. 4 and 5). The core comprises two lithological units (Fig. 7). LU 1 (0–163 cm) contains mottled, irregularly structured, olive-gray sediment with occasional shell fragments and humic particles. Below 75 cm, layers and lenticular structures of coarser sediment become more apparent. At the top (ca. 0–10 cm), the dominant grain sizes are fine and medium sand (25 %–45 %), and the sediment is characterized by poor sorting. Below this, the sediment consists of moderately to poorly sorted fine sand with an average grain size of 73–99 µm. The coarse-grained lens structures and layers consist of fine sand (average grain size 94–102 µm), which is well to moderately well sorted with a symmetrical grain size distribution. Additionally, the sediment contains mixed sections of coarse silt with an average grain size of 32–51 µm, characterized by poorer sorting ($\sigma > 2$) and a fine-skewed grain size distribution. LU 2 (163–366 cm) comprises stratified sands and silts. Layering is due to changes in grain size and color. Coarse-grained layers are irregularly shaped or in the form of lens structures and are characterized by sand contents > 60 % with moderate to poor sorting. The sediment outside these structures is marked by poorly to very poorly sorted, mostly symmetrically distributed grain size distributions with 45 %–70 % silt and 35 %–55 % sand contents. In addition, the sediment features darker-colored layers, suggesting variations in organic content. The deposits were dated to 9134–8966 a cal BP (δ^{13}C–12.20 ‰) at 190 cm and 8985–8687 a cal BP (δ^{13}C–25.28 ‰) at 348 cm (Table 2), indicating an age reversal.

4.2.5 Sediment core EMB382-6-1

Core EMB382-6-1 includes 384 cm of sediment recovered from the low-backscatter platform adjacent to the paleo-river system. The nearest position to a seismic line is plotted in Fig. 4-C1, but, due to the ship changing positions during anchoring for the vibrocorer operation, the core is not directly situated in the profile but is situated instead in a small depression where the uppermost SU is thinning (as observed left to core position in Fig. 4-C1). The core comprises three lithological units with boundaries at 102 and 285 cm (Fig. 7). LU 1 (0–102 cm) displays a coarsening-downward sequence transitioning from coarse silt with fine sand (average grain size of 57 µm) at the top to increasingly poorly sorted fine sands with 19 %–23 % coarse silt, 27 %–38 % fine sand, 25 %–33 % medium sand, and up to 10 % coarse sand at the base. Grain size distributions are symmetrical to fine-skewed. The sediment is marked by a mottled, irregular structure with occasional humic particles in the upper part and shows a distinct interval of darker-colored, organic-rich deposits between 85–102 cm. An erosional unconformity forms the boundary to LU 2, associated with poorly sorted fine- and medium-sandy sediment (average grain size of 255 µm) and gravel components, indicating a high-energy event. LU 2 (102–285 cm) features homogeneous, gray sediment with frequent humic particles. Below ca. 220 cm, remnants of laminations can be recognized, even

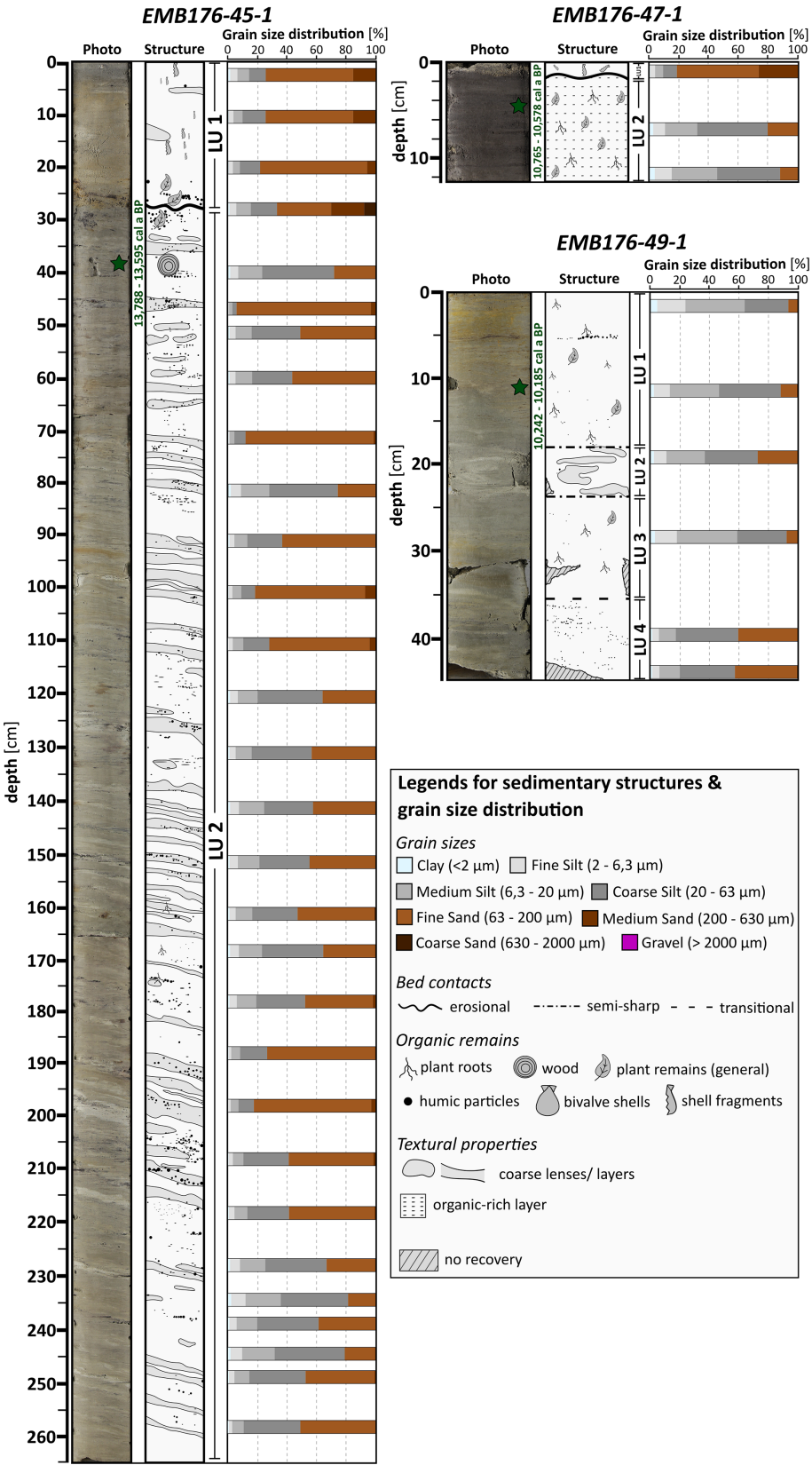


Figure 6. Properties of sediments in cores EMB176-45-1, EMB176-47-1, and EMB176-49-1: core photo, division into lithological units (LUs), sedimentary structures and organic remains, and grain size distribution (%).

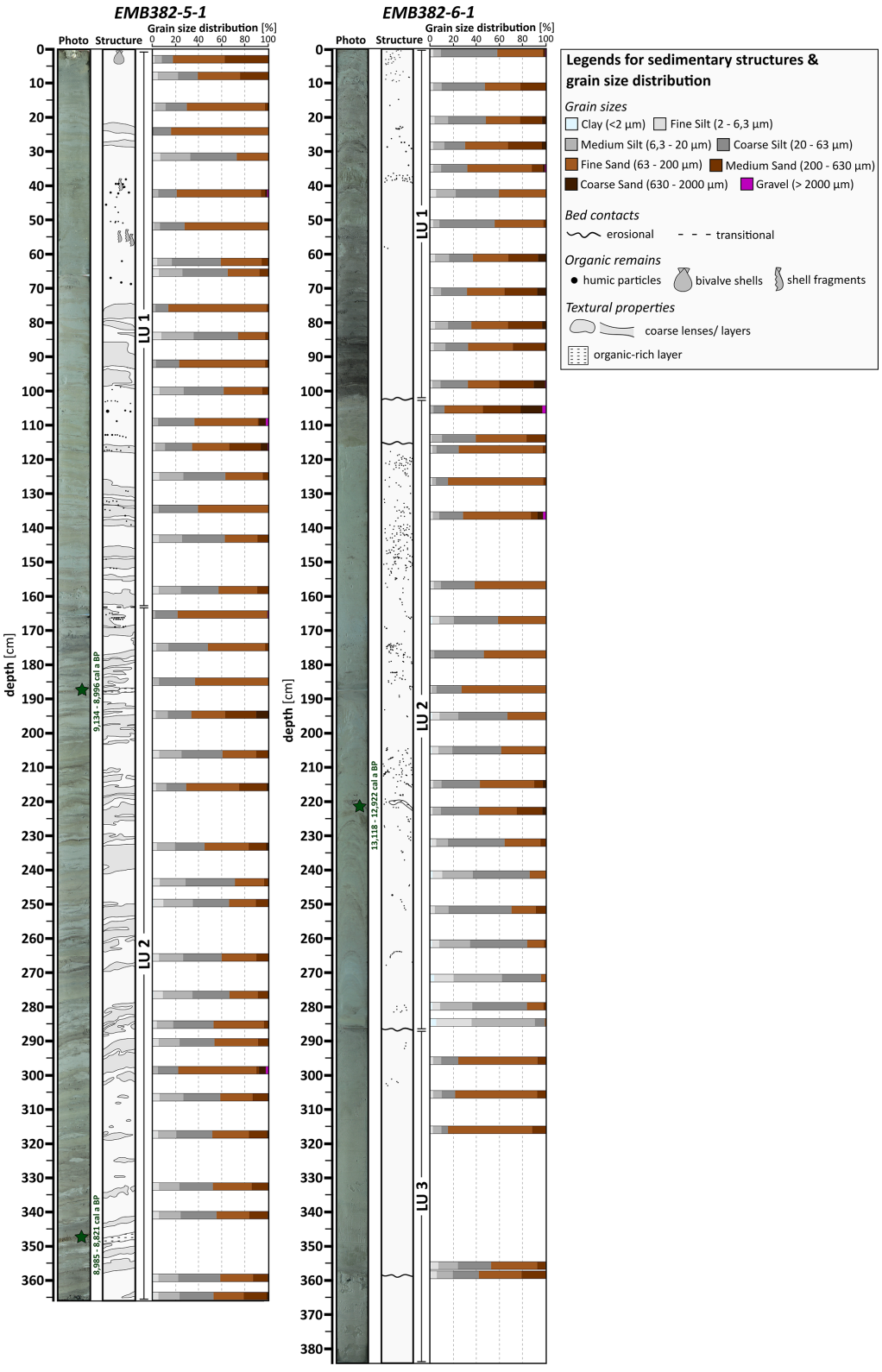


Figure 7. Properties of sediments in cores EMB382-5-1 and EMB382-6-1: core photo, division into lithological units (LUs), sedimentary structures and organic remains, and grain size distribution (%).

though these have been deformed during sampling operations by the vibrocorer. A thin organic-rich layer with plant material at 223 cm has been dated to 13 118–12 922 a cal BP, with a $\delta^{13}C$ value of −26.93 ‰ (Table 2). LU 2 exhibits poorly sorted sediments with a general fining-downward trend from fine sands at the top to medium silts at the base. Below the erosional contact to LU 1, the average grain size is around 90 µm, with dominant coarse-silt (10 %–29 %) and fine-sand (43 %–82 %) grain size fractions. Towards the base, the average grain size decreases to around 20 µm and only 8 µm at the base contact, with dominant medium-silt (12 %–54 %) and coarse-silt (8 %–49 %) contents. An internal unconformity is found at ca. 116 cm within the upper part of LU 2, with brownish deposits overlying olive-gray sediment. Another erosional unconformity delimits LU 2 from LU 3 (285–384 cm), which is composed of homogeneous olive-gray fine sand without internal structures or humic particles. The sediment is poorly sorted with average grain sizes of around 105 and 60 µm in the lower part of the unit, indicating a fining-downward trend below 340 cm. At 360 cm, another erosional contact can be observed, with grain size increasing below to a sandy composition similar to the upper part of the unit.

4.2.6 Video footage

The lateral boundaries of the extensive low-backscatter platform described above (Fig. 2) corresponding to SU 4a, as well as cores EMB176-47-1 and EMB176-49-1 (Fig. 6), have been validated through underwater video imagery from the SINCOS stations 316060, 316090, and 316110 (Fig. 8, the positions of which are marked in Fig. 2a and e). The imagery reveals that the platform is generated by erosional truncation, exposing a remarkably smooth surface. It is made up of densely laminated limnic gyttja deposits with variable sand content beneath (SU 4a). Towards the base, the lamination becomes less pronounced, and the sand content increases based on visual observation and supported by the grain size analysis of core EMB176-49-1, enhancing erodibility. A thin wood fragment in a vertical position protrudes from the seafloor at the base of the sequence at station 316060. While this wood fragment was not sampled, a wood fragment penetrating through the gyttja deposits was radiocarbon-dated to 13 072–12 817 a cal BP at station 316090 (Fig. 8, Table 2). Given the position of the wood fragments in limnic deposits, this fragment was likely redeposited.

4.3 Interpretation of seismic units and stratigraphic relationships

The seismic character of the SU, pointing to different types of sediments, is representative of diverse depositional regimes that prevailed in the study area since the Last Deglaciation. Here, we attempt to provide a relative chronology of the deposits and SUs described in this work based on stratigraphic relationships, the analyzed sediment cores, and correlations with previously described sequences on the Darss Sill and in northeastern Mecklenburg Bay (Lemke and Kuijpers, 1995; Lemke et al., 1998; Bennike and Jensen, 1998; Jensen et al., 2005; Heinrich et al., 2018).

The glacial deposits underlying all Late Glacial and Holocene strata correspond to SU 1 and form the base of acoustic penetration into the subsurface. These deposits crop out at the seafloor adjacent to the Kadet Channel and are characterized by poor sorting, absence of internal stratification, and low seismic penetration, typical of glacial till (Jakobsson et al., 2016). Similar lithologies have been reported in previous studies (Heinrich et al., 2018; Feldens and Schwarzer, 2012).

Overlying the glacial till, postglacial Pleistocene deposits are represented by SU 2 and SU 3 (Bennike and Jensen, 1998; Jensen, 1995). SU 2 displays alternating deformed, laminated sediments and acoustically transparent sections, reflecting the transition from glaciofluvial to early proglacial lake conditions during the onset of the BIL. The sediments were most likely deposited in both lacustrine and terrestrial and/or fluvial environments. Transparent seismic facies, also identified in the Fehmarn Belt (top of seismic unit 1 in Feldens and Schwarzer, 2012), suggest petrophysical homogeneity and stable sedimentation (Sviridov and Emelyanov, 2000). These intervals are interpreted as glaciofluvial sands (Lemke and Kuijpers, 1995; Heinrich et al., 2018), deposited between 17–16 ka cal BP in response to the retreating Weichselian ice margin (Heinrich et al., 2018). The laminated sequences likely represent varved clays and silts of the earliest BIL phases (Zolitschka et al., 2015; Lemke et al., 1998), as also described for the Darss Sill (Lemke and Kuijpers, 1995) and Mecklenburg Bay (seismic unit 3 or sedimentary Unit A1 in Heinrich et al., 2018; unit W2 in Jensen et al., 1997). Sandy deposits sampled in LU 3 of core EMB382-6-1 below 290 cm are in agreement with glaciofluvial sands expected in this unit.

SU 3a corresponds to silty and sandy layers, as well as partly with layers with higher organic content, in LU 2 of core EMB382-6-1. The radiocarbon date of ca. 12.9–13.1 ka cal BP in this section indicates that these sediments were deposited during the initial phase of the Baltic Ice Lake (BILi) and in water depths above ca. 19 m b.s.l. However, the patchy occurrence of the dated plant remains strongly suggests that the material is reworked; therefore, the dates have to be taken with caution. It remains uncertain whether BILf deposits are also present within this unit. An internal unconformity, observed at a depth of 116 cm in core EMB382-6-1, with observable changes in sedimentary composition below and above, could potentially relate to the time interval between different BIL phases; however, this interpretation remains speculative. No material suitable for radiocarbon dating could be acquired in this part of the core, which would be expected for low organic sediments typical of the Baltic Ice Lake sediments deposited in a lacustrine setting (Lemke et al., 1994). The boundary to the overlying deposits in this

Table 2. Radiocarbon dating results used in this study. Water depth is displayed as b.s.l. (below sea level), and sample depths are given as b.s.f (below seafloor). Calendar calibration was performed with the IntCal20 model.

Core/Sample	Lab. no	Position (Lat, long)	Water depth (m b.s.l.)	Sample (cm b.s.f., material)	$\delta^{13}C$ (‰PDB)	^{14}C age (a BP)	Calibrated age (a BP, 2σ range)	Source*
EMB176-45-1	Beta-642373	54.3966, 12.0799	21.4	38–40, wood fragment	−29.0	11 830 ± 40	13 788–13 595	[1]
EMB176-47-1	Beta-642371	54.3756, 12.1104	19.5	3–6, organic-rich sediment	−26.8	9450 ± 30	10 765–10 578	[1]
EMB176-49-1	Beta-642372	54.3743, 12.1670	19.2	11–13, plant material	−9.9	9040 ± 30	10 242–10 185	[1]
EMB382-5-1	Beta-766723	54.3718, 12.1139	19.0	190, plant material	−12.20	8130 ± 30	9134–8996	[1]
EMB382-5-1	Beta-766722	54.3718, 12.1139	19.0	348, plant material	−25.28	7950 ± 30	8985–8821 (48.8 %) 8817–8687 (37.4 %)	[1]
EMB382-6-1	Beta-766721	54.3728, 12.1159	19.6	223, plant material	−26.93	11 130 ± 40	13 118–12 922	[1]
Sincos 316090	–	54.3737, 12.1707	18.5	wood	−25.9	10 992 ± 50	13 072–12 817	[1]
4625/06, HV 18491	DS F 4625/06	54.3775, 12.1519	18.4	16–22, peat	−28.0	9305 ± 165	11 100–10 186	[2]
4625/06, HV 18492	DS F 4625/06	54.3775, 12.1519	18.4	102–106, peat	−30.2	9875 ± 170	11 885–10 991	[2]
560007	AAR-2377	54.5756, 12.2611	19.0	560–573, *Cladium mariscus*	−26.9	9020 ± 130	10 445–9706	[3]
564024	AAR-1919	54.4063, 11.9968	19.0	150–160, *Phragmites australis*	−26.4	9940 ± 110	11 766–11 193	[3]
564024	AAR-2650	54.4063, 11.9968	19.0	70–80, *Carex* sp.	−15.2	9200 ± 90	10 580–10 210	[3]
4775/13 K6341	K-6341	54.3794, 12.1127	20.6	170–175, fen peat (bulk)	−26.3	7800 ± 125	8986–8396	[3]
4775/13 AAR-2651	AAR-2651	54.3794, 12.1127	20.6	170–175, *Nymphaea alba*	−24.1	7940 ± 75	8996–8599	[3]
4775/13 AAR-2373	AAR-2373	54.3794, 12.1127	20.6	170–175, *Cladium mariscus*	−23.8	7820 ± 80	8789–8420	[3]
236	Su-1531	54.26, 11.72	24.6	190–200, *Sphagnum-Bryales* peat	−28.1	9530 ± 80	11 153–10 649	[4]
236	Su-1532	54.26, 11.72	24.6	205–207, *Sphagnum-Bryales* peat	−28.1	9430 ± 100	11 103–10 401	[4]

Note that [1] represents this study, [2] represents Lemke (1998), [3] represents Bennike and Jensen (1998), and [4] Eronen et al. (1990)

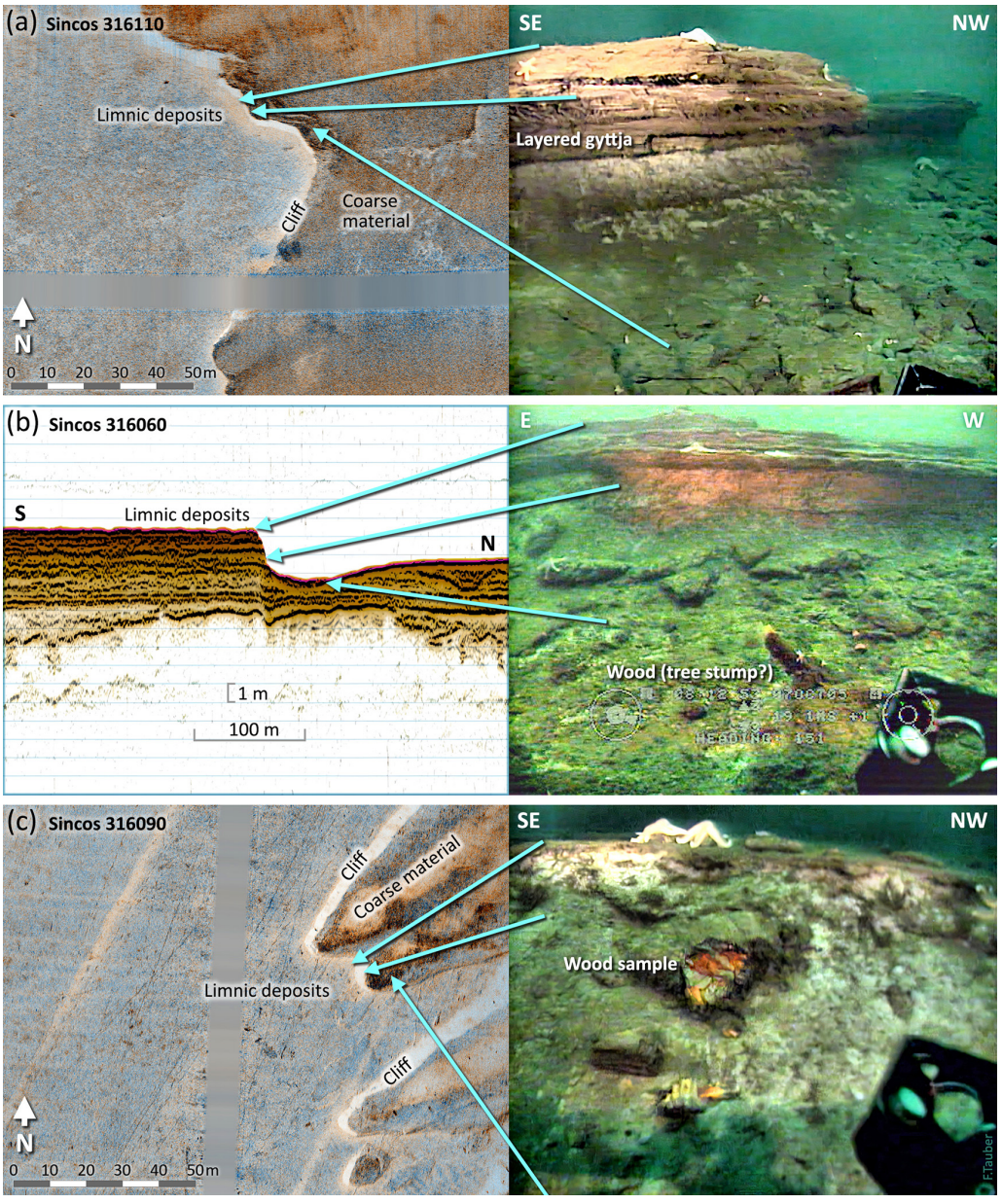


Figure 8. Underwater photography and seismic data for SINCOS stations 316110 **(a)**, 316060 **(b)**, and 316090 **(c)** (for location, refer to Fig. 2), revealing a > 2 m high underwater cliff composed of layered gyttja that corresponds to SU 4a and 3a. The locations of features in the respective photos are marked by arrows. Wood fragments were found in front of the cliff **(b)**, as well as emerging from the seafloor at the base of the exposed SU 3a. The sidescan-sonar images are a combination of two frequencies, with reddish colors indicating dominance of the lower frequency and bluish colors indicating dominance of the higher frequencies. Darker tones refer to higher backscatter intensities.

core is clearly erosive, and the associated gravel content signifies a strong erosive event or period between these two units. This event may have eroded part of the Baltic Ice Lake sediments, leading to an incomplete stratigraphic record at this location.

SU 3b corresponds to stratified sands and silts, observed in core EMB176-45-1 (this study), and lies unconformably above SU 2. Comparable seismic facies have been linked to the lacustrine environment of the BIL in the Arkona Basin (unit E3 in Jensen et al., 1997; Bennike and Jensen, 1998), Mecklenburg Bay (unit W3 in Jensen et al., 1997; Bennike and Jensen, 1998, seismic unit 3 in Heinrich et al., 2018), and the Fehmarn Belt (unit 3 in Novak and Björck, 2004; Feldens and Schwarzer, 2012). The radiocarbon date of ca. 13.6–13.8 ka cal BP from this core (Table 2) indicates deposition during the BILi stage, suggesting a continuous sedimentary sequence during both phases of the BIL. The differences in sedimentological composition and seismic texture

as compared to SU 3a are likely due to water depth; SU 3b represents a more distal location in deeper waters, and SU 3a represents a shallower location proximal to the former shoreline. This can be seen in Fig. 3A, where the acoustic basement of SU 1, which controls the morphology of the Baltic Ice Lake, dips to a depth of more than 28 m b.s.l. (base of acoustic imaging) between the locations of seismic units 3a and 3b.

SU 4 is assigned to Early Holocene deposits related to the AL transgression and regression. These deposits partially crop out at the seafloor and can be observed in backscatter mosaics, underwater imagery, and sediment cores. The upper layers of the laminated gyttja with reduced sand content (and higher resistance to erosion as observed in underwater video images) reflect a deeper and calmer lacustrine environment, suggesting a continuously rising water level and a location further away from the shore (Fig. 9). This is also supported by the fine-grained and organic-rich layers retrieved in cores EMB176-47-1 and EMB176-49-1, even though these cores exhibit notable differences in sedimentological composition, reflecting local-scale variability in depositional patterns. The radiocarbon dates from these cores confirm a deposition throughout the AL transgressive phase (Table 2, Bennike and Jensen, 1998) until at least 10.2 ka cal BP, as determined for core EMB176-49-1 (coinciding with the time of the onset of the AL regression). Due to the $\delta^{13}C$ value of −9.9 ‰ of the aquatic plants in core EMB176-1, the date of 10.2 ka cal BP may be an overestimation, and it cannot be ruled out that lake conditions prevailed for longer in the study site. However, similar radiocarbon dating is described by Jensen et al. (1999) and Bennike and Jensen (1998) in cores 560007 (eastern Darss Sill) and 564024 (ca. 2 km west of the study site), which contain faintly laminated freshwater sands with plant remains, dated to ca. 10.1 and ca. 10.4 ka cal BP, respectively (Table 2). Further age confirmation is derived from samples HV 18491 and HV 18492 in core 4625/06, as reported by Lemke (1998), who recovered peat material from the low-backscatter platform (marked in Fig. 2) at depths of 16–22 and 102–106 cm below seafloor and yielded ages of 11.1–10.2 and 11.9–11.0 ka cal BP (Table 2). The widespread, spatially coherent, and laminated nature of SU 4a, sampled in cores EMB176-47-1 and EMB176-49-1 and imaged in acoustic data, rules out an interpretation as organic detritus as reported in deeper Mecklenburg Bay environments (Bennike and Jensen, 1998). Instead, the sediments were probably accumulated in a lacustrine environment as a response to rising groundwater levels due to the AL transgression, partly forming gyttja deposits, as has been described in the southwestern Arkona Basin (Lemke and Kuijpers, 1995; Bennike and Jensen, 1998), on the Falster–Rügen sand plain (Lemke et al., 2001), and in central Mecklenburg Bay (Eronen et al., 1990).

SU 4b, consisting of inclined-strata infilling-incised channels, was sampled and dated in section 2 of core EMB382-5-1. The succession of younger ages below older ages in core EMB382-5-1 suggests intense reworking of sediment. Nevertheless, the maximum age of the channel infill is constrained by both datings to 9.0 ka cal BP, coinciding with the time after the AL regression (Jensen et al., 1999). Additional age control is derived from radiocarbon dates in core 4775/13 (Bennike and Jensen, 1998) on a sharply delimited section of compacted peat gyttja with plant remains at a depth of 170–175 cm (samples K6341, AAR-2373, and AAR-2651), yielding ages between 8.6 and 8.8 ka cal BP (Table 2). This core was recovered in direct proximity to the eastern branch of the channel system described here (Fig. 2) and should have, therefore, sampled the adjacent older deposits of SU 4a and 3a. The reported ages for this core (Bennike and Jensen, 1998) are, however, contradictory to the surface age of the samples from SU 4a (10.2 ka cal BP in core EMB176-49-1). We therefore suggest that, due to the uncertainty of navigation systems at that time, the core, in fact, sampled the channel system of SU 4b and, thus, the time it was inactive and filled with AL period deposits. This is also supported by the similar age in core EMB382-5-1. Both ages together (Table 2) therefore show that the channel infill postdates the maximum transgression of the AL.

SU 5, sampled in LU 1 of cores EMB176-45-1 and EMB176-47-1, represents bioturbated sandy sediments deposited since the onset of the Littorina Transgression (Virtasalo et al., 2016). These deposits are widespread in the Baltic Sea basins below 20 m depth. The N–S-trending dune system likely formed from the onset of the Littorina Transgression, but no age control is available. SU 5 is not further discussed in this study.

5 Discussion

The postglacial geological evolution of the Baltic Sea reflects the interplay of climate change, shore-level dynamics, and regional paleoenvironmental shifts since the Last Glacial Maximum. During the Late Pleistocene–Holocene transition, the region underwent rapid transformations – evolving from ice-covered landscapes to lake and river landscapes, followed by the establishment of the brackish marine Baltic basin. The reconstruction of past water levels and shoreline positions, the nature and timing of the Baltic Ice Lake and Ancylus Lake stages, understanding the development of drainage networks, and assessing the implications for human settlements throughout northern Europe are central research themes in the geological study of the Baltic Sea.

The spatial distribution of Baltic Ice Lake deposits in the study area constrains the paleo-water levels during the initial phase of the BIL, with a coastline being inferred close to the core locations. The proximity to the coastline during the BILi period is supported by sedimentological and radiocarbon data of core EMB176-45-1 and core EMB382-6-1, which sampled a proximal, near-coastal area of the ice lake. In contrast to the findings of varved clays east of the

Darss Sill (Jensen and Stecher, 1992; Lemke et al., 1994), central Mecklenburg Bay (Kostecki et al., 2015; Heinrich et al., 2018), or the Arkona Basin (Bennike and Jensen, 1998), which represent more shore-distal deposits, the sediments sampled in these cores consist of coarser-grained deposits without a clear varve structure. The humic particles, wood fragments, and organic layers have probably been transported over short distances from a nearby land area. An in situ formation of the organic layers in core EMB176-45-1 and core EMB382-6-1 is unlikely due to their poor preservation and the reported overall lack of organic material in BIL deposits (Lemke et al., 1994; Moros et al., 2002; Heinrich et al., 2018). A similar relationship between geographical position and sedimentological composition has been described in Faxe Bugt, where a coastline of the BILf was identified (Jensen and Stecher, 1992; Bennike and Jensen, 1995). Further support for the coastal proximity during the BIL period derives from observations of in situ wood remnants (Fig. 8), suggesting terrestrial conditions at or near the sites of Fig. 8. The radiocarbon dates of the terrestrial wood (ca. 13.6–13.8 ka cal BP) and the plant fragments (ca. 12.9–13.1 ka cal BP; Table 2) within SU 3a correspond to the late BILi period, similarly to the layered deposits observed in deeper water of 20 m b.s.l. (SU 3b). This requires a paleo-shoreline between these two sites. A paleo-shoreline in the study area at a maximum water level of 20–21 m b.s.l. is consistent with the maximum water level of the BIL in Mecklenburg Bay (Bennike and Jensen, 1998) and the depth levels described by Heinrich et al. (2018). The findings further confirm a connection between these areas and the southwestern Arkona Basin east of the Darss Sill threshold during the BIL, likely during its initial phase (Lampe, 2005, Fig. 9). The maximum water level of the final BIL cannot be further constrained with the data presented here as we cannot attribute any sediments specifically to the BILf period.

The unconformity at the top of SU 3 marks a significant post-BIL event and widespread erosion in the investigation site. The erosional unconformity is not associated with recent high bottom velocities able to remobilize bottom sediments, such as those experienced during significant inflow events (Zhurbas et al., 2018) through the Kadet Channel, as the unconformity is partially overlain by sediments of the Littorina period (Fig. 3, LU 1 in core EMB176-45-1). A similar stratigraphic relationship has also been described by Jensen et al. (1997) in core MB03/94, ca. 20 km west of the study area, and by Bennike and Jensen (1998), who noticed a hiatus between freshwater and LS deposits in coastal areas of Mecklenburg Bay. The upper limit for the timing of the erosional activity is 13.5 ka cal BP, based on the sample in core EMB176-45-1, ca. 10 cm below the unconformity (this study). In western Mecklenburg Bay, approximately 20 km west of the Darss Sill, Heinrich et al. (2018) documented a similar large-scale erosional unconformity that cuts the last Baltic Ice Lake deposits at an age of ca. 10.7–11.6 ka cal BP, coinciding with the time between the BILf regression and the YS lowstand (Lampe, 2005). The age for this unconformity found in our study thus contradicts the age from Heinrich et al. (2018). However, the dip of the strata near core EMB176-45-1 (Fig. 3) suggests that the core did not capture the most recent deposits below the unconformity, explaining the older age observed in this study. In addition to widespread erosional activity between the two BIL phases, Heinrich et al. (2018) noticed patchy remnants of YS-aged lowstand fluvial deposits in seismic lines at depths of 30 m b.s.l. in western Mecklenburg Bay. The absence of similar YS deposits at our site below 20 m b.s.l. may be due to incomplete seismic coverage (although such features would be expected to be visible in backscatter mosaics of the seafloor) or complete erosion closer to the Darss Sill. In any case, we conclude that a phase of erosion occurred around the time of the BIL regression and/or YS lowstand in the study area.

Evidence for a second erosive event, occurring after the AL highstand, can be inferred from the partially preserved limnic deposits deposited in a near-shore position in water depths of 19 m b.s.l. These deposits constrain the upper limit for the maximum water level during the AL transgression in eastern Mecklenburg Bay. A similar water level was reconstructed in previous studies in the same region (Lemke et al., 1994, 1998; Jensen et al., 1997, 1999; Bennike and Jensen, 1998; Kostecki et al., 2015). Notably, the youngest deposits dated to the AL period coincide with the beginning of the AL regression (Table 2), suggesting that erosion on top of the platform was limited after the AL regression (in contrast to the erosion following the BIL, which removed a larger part of the sedimentary sequence). Instead, the erosion focused on cliffs as observed in video images (Fig. 8). Nevertheless, based on the presented data, this erosion cannot be attributed to a certain time period, and we cannot rule out that erosion is still ongoing in the present day.

A terrestrial fluvial system eroded into the AL and older deposits, imaged by SU 4b, provides evidence for significant water level fluctuations following the AL highstand (Table 1). In total, three continuous branches of this fluvial system can be recognized in bathymetric and sediment echo sounder data (Fig. 4). Occasionally, the channel rims form local seafloor elevations, also observed on the northeastern Darss Sill by Tauber (2011). This is caused by the higher erosive resistance of the more cohesive, organic-rich deposits compared to the underlying sandy gyttja as observed in video footage (Fig. 8), also described by Tauber (2011) for peat ridges marking the path of a former fluvial channel. However, there is no discernible pattern in the preservation of the elevated areas of the river channels in relation to their water depth or morphological patterns. The preserved elevated areas appear to be the result of random erosion processes.

As the channel system is incised down to 25–26 m b.s.l. (Fig. 5) and because the complete infill consists of AL-period deposits (core EMB382-5-1), a water level drop of at least 6–7 m must have occurred between the deposition of the limnic deposits and the formation of the channel. The

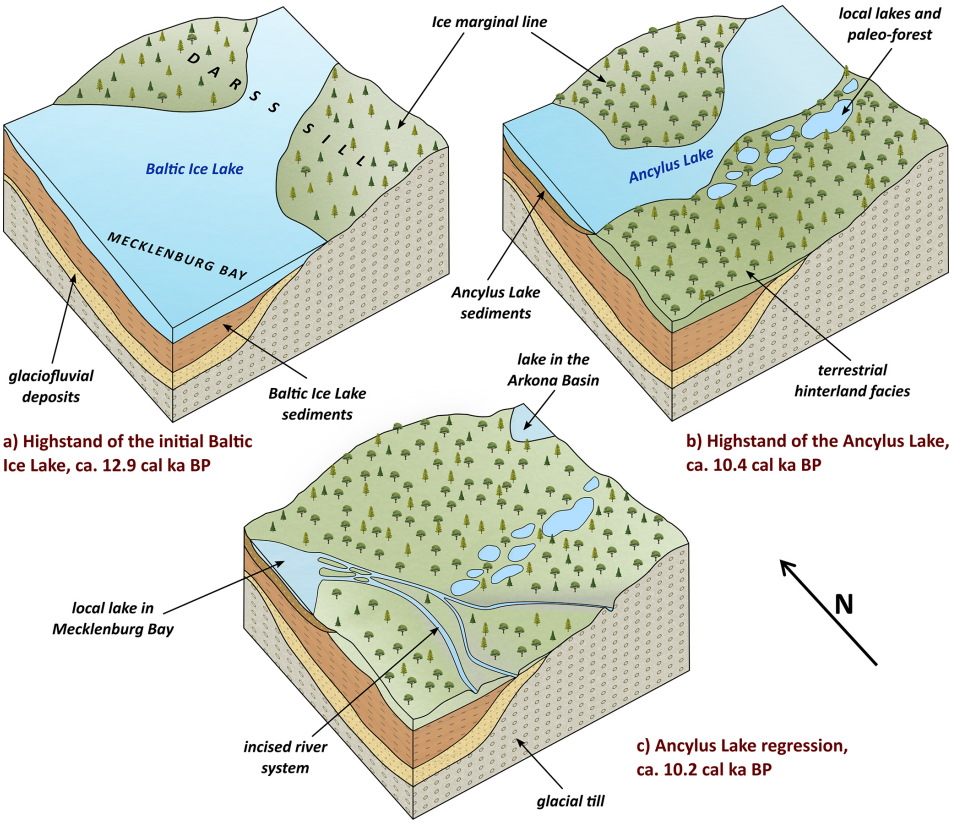


Figure 9. Paleogeographic reconstruction of the study area during the **(a)** Baltic Ice Lake highstand, **(b)** Ancylus Lake highstand, and **(c)** regression following the Ancylus Lake highstand.

timing of this regression is constrained by the radiocarbon dates of ca. 8.7–9.0 ka cal BP, observed in the channels at depths of over 1 m. Consequently, the water level drop must have occurred during the period between the AL highstand at ca. 10.4 ka cal BP (Fig. 9) and the time when the Littorina Transgression reached a water level of 25–26 m b.s.l. and flooded the channel base at ca. 9 to 8.5 ka cal BP (Bennike and Jensen, 1998). In this context, a genetic link to the AL regression is reasonable as channel formation usually occurs during sea level drops (Talling, 1998). During the following Littorina Transgression, depressions along the channel pathway were likely filled with the sandy sediments observed in LU 1 of core EMB382-5-1, although no age control is available for this unit. A water level drop of 6–7 m is consistent with the value proposed by Bennike and Jensen (1998) and later by Björck et al. (2008) to reconcile theories of the Ancylus Lake regression in the Darss Sill area. There is no indication of a large east–west-trending Dana River channel in this study.

The limnic deposits of the AL period at 19 m b.s.l. consequently support the fact that the Darss Sill was flooded during the AL highstand at ca. 10.4 ka cal BP (Lemke et al., 2002a; Fig. 9). Accordingly, the critical threshold restricting this dammed lake must have been situated further west if the Great Belt was the main pathway of AL regression outflow (Feldens and Schwarzer, 2012; Bendixen et al., 2017) since thresholds further to the east are located at 23–24 m b.s.l. (Lemke et al., 2001). The channel system described in this study can be tracked down to a maximum water depth of 22 m b.s.l. in the northwest of the study area. However, based on the available data, it is not possible to determine where the channel system flows into the remaining lake body following the AL regression, which should correspond to the local water level following the AL regression that determined whether a connection through the Kadet Channel existed after the AL regression. North of the Kadet Channel, remnants of similar channel systems can be traced down to a depth of 23.5 m b.s.l. (Tauber, 2011), which corresponds to the depth of the threshold in the Kadet Channel of 23–24 m b.s.l. (Lemke et al., 2001). The observed, widespread erosion of SU 3a and 4a, as widely observed in seismic and bathymetric data and sampled by cores EMB176-45-1 and EMB382-6-1, is in contrast to previous reports of absent Holocene erosional features on the Darss Sill (Bennike and Jensen, 1998; Lemke et al., 1999). However, it remains uncertain whether this erosion occurred during the AL regression and subsequent lowstand or during the period of the initial Littorina Transgression as a result of changed near-bottom currents,

redistribution of sediments, or decreased sediment supply, as suggested by Virtasalo et al. (2016).

6 Conclusions

Integrating seismic, sedimentological, and radiocarbon data provides a detailed reconstruction of the paleogeography in the study area through the Baltic Ice Lake (BIL) and Ancylus Lake (AL) periods. The data support a paleo-coastline of the BIL at 20–21 m below present sea level (b.s.l.) in northeastern Mecklenburg Bay. The seismic data provide no evidence of an erosional unconformity dividing the BIL deposits into an initial and final stage; however, a widespread post-BIL erosional unconformity was identified. The maximum water level of the AL was reconstructed to 19 m b.s.l. based on the occurrence of lacustrine sediments. During that time, an environment of small, local lakes was present on the threshold. The formation of a river system and fluvial incision suggests a water-level drop of 6–7 m following the AL highstand, indicating a moderate AL regression rather than catastrophic drainage. We conclude that extensive erosion occurred on the Darss Sill in the Holocene. The water levels reconstructed for the BIL and AL maximum transgressions support a flooding of the Darss Sill. Nevertheless, the drainage route of the AL and the formation and role of the Kadet Channel during these transgressions and regressions are still unsolved. To reconcile this, future studies should address the water level development directly east of the Darss Sill. The dataset presented here demonstrates the widespread preservation of paleo-landscapes in the Baltic Sea, with potential for further paleogeographical and archeological investigations from the coastline to 20 m water depth along the southern Baltic Sea.

Data availability. Sidescan-sonar data, seismic lines, and grain size information are available from Zenodo, https://doi.org/10.5281/zenodo.14887536 (Feldens, 2025). Bathymetric data of the investigation site are available for download from the Federal Maritime Agency of Germany (BSH).

Sample availability. Sediment cores are stored in the core storage facilities of the Leibniz Institute for Baltic Sea Research Warnemünde. Material from the sediment cores is available upon request.

Author contributions. Conceptualization: PF. Data curation: PF. Investigation: JG, PF, FT, HWA. Funding acquisition: PF. Methodology: PF, HWA, FT, JG. Project administration: PF. Resources: HWA, PF. Software: FT, PF. Supervision: HWA, PF. Visualization: JG, FT, PF. Writing (original draft preparation): JG, PF. Writing (review and editing): JGE, FT, HWA.

Competing interests. The contact author has declared that none of the authors has any competing interests.

Disclaimer. Publisher's note: Copernicus Publications remains neutral with regard to jurisdictional claims made in the text, published maps, institutional affiliations, or any other geographical representation in this paper. The authors bear the ultimate responsibility for providing appropriate place names. Views expressed in the text are those of the authors and do not necessarily reflect the views of the publisher.

Acknowledgements. We thank the captain and crew of RV *Elisabeth Mann Borgese* for their perfect support during our work. We are grateful to Mischa Schönke, Inken Schulze, and Jerome Kaiser for their assistance. Lastly, we greatly appreciate the technical help provided by Andreas Frahm, Mike Sommer, and Martin Karallus during the sampling and survey activities. We thank all of the scientists and technicians involved in the SINCOS project, who recorded sidescan-sonar and video data from 2005 to 2008. We appreciate the thorough and constructive comments of the two reviewers that substantially improved the paper.

Review statement. This paper was edited by Markus Fuchs and reviewed by two anonymous referees.

References

Andrén, E., Andrén, T., and Sohlenius, G.: The Holocene history of the southwestern Baltic Sea as reflected in a sediment core from the Bornholm Basin, Boreas, 29, 233–250, https://doi.org/10.1111/j.1502-3885.2000.tb00981.x, 2000.

Andrén, T., Lindeberg, G., and Andrén, E.: Evidence of the final drainage of the Baltic Ice Lake and the brackish phase of the Yoldia Sea in glacial varves from the Baltic Sea, Boreas, 31, 226–238, 2002.

Andrén, T., Björck, S., Andrén, E., Conley, D., Zillén, L., and Anjar, J.: The Development of the Baltic Sea Basin During the Last 130 ka, in: The Baltic Sea Basin, edited by: Harff, J., Björck, S., and Hoth, P., pp. 75–97, Springer, Berlin, Heidelberg, ISBN 978-3-642-17220-5, https://doi.org/10.1007/978-3-642-17220-5_4, 2011.

Bendixen, C., Jensen, J. B., Boldreel, L. O., Clausen, O. R., Bennike, O., Seidenkrantz, M.-S., Nyberg, J., and Hübscher, C.: The Holocene Great Belt connection to the southern Kattegat, Scandinavia: Ancylus Lake drainage and Early Littorina Sea transgression, Boreas, 46, 53–68, https://doi.org/10.1111/bor.12154, publisher: Wiley, 2017.

Bennike, O. and Jensen, J. B.: Near-shore Baltic Ice Lake deposits in Fakse Bugt, southeast Denmark, Boreas, 24, 185–195, https://doi.org/10.1111/j.1502-3885.1995.tb00772.x, 1995.

Bennike, O. and Jensen, J. B.: Late- and postglacial shore level changes in the southwestern Baltic Sea, B. Geol. Soc. Denmark, 45, 27–38, https://doi.org/10.37570/bgsd-1998-45-04, 1998.

Bennike, O. and Jensen, J. B.: A Baltic Ice Lake lowstand of latest Alleröd age in the Arkona Basin, southern Baltic Sea, GEUS

Bulletin, 28, 17–20, https://doi.org/10.34194/geusb.v28.4710, 2013.

Bennike, O., Lemke, W., and Jensen, J. B.: Fauna and flora in submarine early Holocene lake-marl deposits from the southwestern Baltic Sea, The Holocene, 8, 353–358, https://doi.org/10.1191/095968398673688465, 1998.

Bennike, O., Jensen, J. B., Lemke, W., Kuijpers, A., and Lomholt, S.: Late- and postglacial history of the Great Belt, Denmark, Boreas, 33, 18–33, https://doi.org/10.1080/03009480310006952, 2004.

Bennike, O., Jensen, J. B., Nörgaard-Pedersen, N., Andresen, K. J., Seidenkrantz, M.-S., Moros, M., and Wagner, B.: When were the straits between the Baltic Sea and the Kattegat inundated by the sea during the Holocene?, Boreas, 50, 1079–1094, https://doi.org/10.1111/bor.12525, 2021.

Björck, S.: A review of the history of the Baltic Sea, 13.0–8.0 ka BP, Quat. Int., 27, 19–40, 1995.

Björck, S.: The late Quaternary development of the Baltic Sea basin, Assessment of Climate Change for the Baltic Sea Basin, pp. 398–407, ISBN 978-3-540-72785-9, 2008.

Björck, S. and Digerfeldt, G.: Climatic Changes at Pleistocene/Holocene Boundary in the Middle Swedish Endmoraine Zone, Mainly Inferred from Stratigraphic Indications, in: Climatic Changes on a Yearly to Millennial Basis: Geological, Historical and Instrumental Records, edited by: Mörner, N.-A. and Karlén, W., pp. 37–56, Springer Netherlands, Dordrecht, ISBN 978-94-015-7692-5, https://doi.org/10.1007/978-94-015-7692-5_4, 1984.

Björck, S. and Digerfeldt, G.: Alleröd- Younger Dryas sea level changes in southwestern Sweden and their relation to the Baltic Ice Lake development, Boreas, 20, 115–133, https://doi.org/10.1111/j.1502-3885.1991.tb00301.x, 1991.

Björck, S., Andrén, T., and Jensen, J. B.: An attempt to resolve the partly conflicting data and ideas on the Ancylus–Littorina transition, Pol. Geol. Inst. Spec. Pap., 23, 21–26, 2008.

Blott, S. J. and Pye, K.: GRADISTAT: a grain size distribution and statistics package for the analysis of unconsolidated sediments, Earth Surf. Process. Landf., 26, 1237–1248, https://doi.org/10.1002/esp.261, 2001.

Eronen, M., Ristaniemi, O., and Lange, D.: Analysis of a sediment core from the Mecklenburg Bay, with a discussion on the early Holocene history of the southern Baltic Sea, Geol. Foereningan Stockh. Foerhandlingar, 112, 1–8, https://doi.org/10.1080/11035899009453155, 1990.

Feldens, P.: Dataset regarding the Paleogeography of a lake and river system in north-eastern Mecklenburg Bay, southern Baltic Sea, Zenodo [data set], https://doi.org/10.5281/zenodo.14887536, 2025.

Feldens, P. and Schwarzer, K.: The Ancylus Lake stage of the Baltic Sea in Fehmarn Belt: Indications of a new threshold?, Cont. Shelf Res., 35, 43–52, https://doi.org/10.1016/j.csr.2011.12.007, 2012.

Geersen, J., Bradtmöller, M., Schneider von Deimling, J., Feldens, P., Auer, J., Held, P., Lohrberg, A., Supka, R., Hoffmann, J. J. L., Eriksen, B. V., Rabbel, W., Karlsen, H.-J., Krastel, S., Brandt, D., Heuskin, D., and Lübke, H.: A submerged Stone Age hunting architecture from the Western Baltic Sea, P. Natl. Acad. Sci. USA, 121, e2312008121, https://doi.org/10.1073/pnas.2312008121, 2024.

Godwin, H.: Half-life of Radiocarbon, Nature, 195, 984–984, https://doi.org/10.1038/195984a0, 1962.

Gustafsson, B. G. and Westman, P.: On the causes for salinity variations in the Baltic Sea during the last 8500 years, Paleoceanography, 17, 12-1–12-14, https://doi.org/10.1029/2000PA000572, 2002.

Hansson, A., Nilsson, B., Sjöström, A., Björck, S., Holmgren, S., Linderson, H., Magnell, O., Rundgren, M., and Hammarlund, D.: A submerged Mesolithic lagoonal landscape in the Baltic Sea, south-eastern Sweden – Early Holocene environmental reconstruction and shore-level displacement based on a multiproxy approach, Quat. Int., 463, 110–123, https://doi.org/10.1016/j.quaint.2016.07.059, 2018.

Harff, J., Björck, S., and Hoth, P. (Eds.): The Baltic Sea Basin, Central and Eastern European Development Studies (CEEDES), Springer Berlin Heidelberg, Berlin, Heidelberg, ISBN 978-3-642-17219-9 978-3-642-17220-5, https://doi.org/10.1007/978-3-642-17220-5, 2011.

Harff, J., Deng, J., Dudzińska-Nowak, J., Fröhle, P., Groh, A., Hünicke, B., Soomere, T., and Zhang, W.: Coastline Changes of the Baltic Sea from South to East, Coastal Research Library, pp. 15–35, https://doi.org/10.1007/978-3-319-49894-2_2, 2017.

Heinrich, C., Anders, S., and Schwarzer, K.: Late Pleistocene and early Holocene drainage events in the eastern Fehmarn Belt and Mecklenburg Bight, Baltic Sea, Boreas, 47, 754–767, https://doi.org/10.1111/bor.12298, 2018.

Hoffmann, G., Schmedemann, N., and Schafmeister, M.-T.: Relative sea-level curve for SE Rügen and Usedom Island (SW Baltic Sea coast, Germany) using decompacted profiles, Zeitschrift der Deutschen Gesellschaft für Geowissenschaften, 160, 69–78, https://doi.org/10.1127/1860-1804/2009/0160-0069, 2009.

Hughes, A. L. C., Gyllencreutz, R., Lohne, Ã. S., Mangerud, J., and Svendsen, J. I.: The last Eurasian ice sheets – a chronological database and time-slice reconstruction, DATED-1., Boreas, 45, 1–45, https://doi.org/10.1111/bor.12142, 2016.

Jakobsson, M., Björck, S., Alm, G., Andrén, T., Lindeberg, G., and Svensson, N.-O.: Reconstructing the Younger Dryas ice dammed lake in the Baltic Basin: Bathymetry, area and volume, Glob. Planet. Change, 57, 355–370, https://doi.org/10.1016/j.gloplacha.2007.01.006, 2007.

Jakobsson, M., Gyllencreutz, R., Mayer, L. A., Dowdeswell, J. A., Canals, M., Todd, B. J., Dowdeswell, E. K., Hogan, K. A., and Larter, R. D.: Mapping submarine glacial landforms using acoustic methods, Geological Society, London, Memoirs, 46, 17–40, https://doi.org/10.1144/M46.182, 2016.

Jensen, J. B.: A Baltic Ice Lake transgression in the southwestern Baltic: Evidence from Fakse Bugt, Denmark, Quat. Int., 27, 59–68, https://doi.org/10.1016/1040-6182(94)00061-9, 1995.

Jensen, J. B. and Stecher, O.: Paraglacial barrier-lagoon development in the late pleistocene Baltic Ice Lake, southwestern Baltic, Mar. Geol., 107, 81–101, 1992.

Jensen, J. B., Bennike, O., Witkowski, A., Lemke, W., and Kuijpers, A.: The Baltic Ice Lake in the southwestern Baltic: sequence. chrono. and biostratigraphy, Boreas, 26, 217–236, https://doi.org/10.1111/j.1502-3885.1997.tb00853.x, 1997.

Jensen, J. B., Bennike, O., Witkowski, A., Lemke, W., and Kuijpers, A.: Early Holocene history of the southwestern Baltic Sea: the Ancylus Lake stage, Boreas, 28, 437–453, https://doi.org/10.1111/j.1502-3885.1999.tb00233.x, 1999.

Jensen, J. B., Bennike, O., Lemke, W., and Kuijpers, A.: The Storebælt gateway to the Baltic, Geol. Surv. Den. Greenl. Bull., 7, 45–48, https://doi.org/10.34194/geusb.v7.4831, 2005.

Johnson, M. D., Kylander, M. E., Casserstedt, L., Wiborgh, H., and Björck, S.: Varved glaciomarine clay in central Sweden before and after the Baltic Ice Lake drainage: a further clue to the drainage events at Mt Billingen, GFF, 135, 293–307, https://doi.org/10.1080/11035897.2013.819032, 2013.

Kaiser, K.: Die spätpleistozäne bis frühholozäne Beckenentwicklung in Mecklenburg-Vorpommern: Untersuchungen zur Stratigraphie, Geomorphologie und Geoarchäologie, no. 24 in Greifswalder geographische Arbeiten, Ernst-Moritz-Arndt-Univ. Greifswald, Greifswald, ISBN 978-3-86006-183-1, 2001.

Kolp, O.: Paläogeographische Ergebnisse der Kartierung des Meeresgrundes der westlichen Ostsee zwischen Fehmarn und Arkona, Akademie Verlag, 19–59 pp., 1965.

Kolp, O.: Entwicklungsphasen des Ancylus-Sees (Phases d'évolution du lac – Ancylus), Petermanns Geogr. Mitt., 130, 79–94, https://pascal-francis.inist.fr/vibad/index.php?action=getRecordDetail&idt=12061994 (last access: 10 February 2026), 1986.

Kostecki, R., Janczak-Kostecka, B., Endler, M., and Moros, M.: The evolution of the Mecklenburg Bay environment in the Holocene in the light of multidisciplinary investigations of the sediment cores, Quat. Int., 386, https://doi.org/10.1016/j.quaint.2015.07.007, 2015.

Lambeck, K.: Shoreline displacements in southern-central Sweden and the evolution of the Baltic Sea since the last maximum glaciation, J. Geol. Soc., 156, 465–486, https://doi.org/10.1144/gsjgs.156.3.0465, 1999.

Lambeck, K. and Chappell, J.: Sea Level Change Through the Last Glacial Cycle, Science, 292, 679–686, https://doi.org/10.1126/science.1059549, 2001.

Lampe, R.: Lateglacial and Holocene water-level variations along the NE German Baltic Sea coast: review and new results, Quat. Int., 133–134, 121–136, https://doi.org/10.1016/j.quaint.2004.10.005, 2005.

Lampe, R., Naumann, M., Meyer, H., Janke, W., and Ziekur, R.: Holocene evolution of the southern Baltic sea coast and interplay of sea-level variation, isostasy, accommodation and sediment supply, in: The Baltic Sea Basin, pp. 233–251, Springer Berlin Heidelberg, Berlin, Heidelberg, ISBN 978-3-642-17219-9, https://doi.org/10.1007/978-3-642-17220-5_12, 2011.

Lemke, W.: Sedimentation und paläogeographische Entwicklung im westlichen Ostseeraum (Mecklenburger Bucht bis Arkonabecken) vom Ende der Weichselvereisung bis zur Litorinatransgression, Meereswissenschaftliche Berichte, Institut für Ostseeforschung Warnemünde, 31, pp. 156, https://www.iow.de/files/forschung/meereswissenschaftliche-berichte/mebe31_1998_lemke.pdf (last access: 4 June 2026), 1998.

Lemke, W. and Kuijpers, A.: Late Pleistocene and early Holocene paleogeography of the Darss Sill area, southwestern Baltic, Quat. Int., 27, 73–81, 1995.

Lemke, W., Kuijpers, A., Hoffmann, G., Milkert, D., and Atzler, R.: The Darss Sill, hydrographic threshold in the southwestern Baltic: Late Quaternary geology and recent sediment dynamics, Cont. Shelf Res., 14, 847–870, 1994.

Lemke, W., Jensen, J. B., Bennike, O., and Witkowski, A.: Sequence stratigraphy of submarine late pleistocene and holocene deposits in mecklenburg bay, south-western baltic, Sveriges Geol. Undersögning Ca., 86, 117–122, 1997.

Lemke, W., Endler, R., Tauber, F., Jensen, J. B., and Bennike, O.: Late- and postglacial sedimentation in the Tromper Wiek northeast of Rügen (western Baltic), Meyniana, 50, 155–173, 1998.

Lemke, W., Jensen, J. B., Bennike, O., Witkowski, A., and Kuijpers, A.: No indication of a deeply incised Dana River between Arkona Basin and Mecklenburg Bay, Baltica, 12, 66, 1999.

Lemke, W., Jensen, J. B., Bennike, O., Endler, R., Witkowski, A., and Kuijpers, A.: Hydrographic thresholds in the western Baltic Sea: Late Quaternary geology and the Dana River concept, Mar. Geol., 176, 191–201, https://doi.org/10.1016/s0025-3227(01)00152-9, 2001.

Lemke, W., Jensen, J. B., Bennike, O., Endler, R., Witkowksi, A., and Kuijpers, A.: Spät- und postglaziale Flüsse und Seen in der heutigen westlichen Ostsee, Greifswalder Geographische Arbeiten, 26, 73–77, 2002a.

Lemke, W., Schwarzer, K., and Diesing, M.: Quaternary development of Tromper Wiek, Rügen island, Greifswalder Geographische Arbeiten, 27, 61–67, 2002b.

Lohne, Ã. S., Mangerud, J., and Svendsen, J. I.: Timing of the younger dryas glacial maximum in western Norway, J. Quaternary Sci., 27, 81–88, https://doi.org/10.1002/jqs.1516, 2012.

Lohne, S., Mangerud, J., and Birks, H. H.: Precise 14C ages of the Vedde and Saksunarvatn ashes and the Younger Dryas boundaries from western Norway and their comparison with the Greenland Ice Core (GICC05) chronology, J. Quaternary Sci., 28, 490–500, https://doi.org/10.1002/jqs.2640, 2013.

Mörner, N.-A.: The northwest European "sea-level laboratory" and regional holocene eustasy, Palaeogeogr. Palaeoclimatol. Palaeoecol., 29, 281–300, https://doi.org/10.1016/0031-0182(79)90086-5, 1979.

Moros, M., Lemke, W., Kuijpers, A., Endler, R., Jensen, J. B., Bennike, O., and Gingele, F.: Regressions and transgressions of the Baltic basin rejected by a new high-resolution deglacial and postglacial lithostratigraphy for Arkona Basin sediments (western Baltic Sea), 31, 151–162, 2002.

Munsell, A. H.: Munsell soil color charts, Gretagmacbeth, 2000.

Naughton, F., Sánchez-Goñi, M. F., Landais, A., Rodrigues, T., Riveiros, N. V., and Toucanne, S.: Chapter 6 – The Bølling-Alleröd Interstadial, in: European Glacial Landscapes, edited by Palacios, D., Hughes, P. D., García-Ruiz, J. M., and Andrés, N., pp. 45–50, Elsevier, ISBN 978-0-323-91899-2, https://doi.org/10.1016/B978-0-323-91899-2.00015-2, 2023.

Novak, B. and Björck, S.: Marine seismic studies in southern Kattegat, with special emphasis on longitudinal bars and their possible relationship to the drainage of the Ancylus Lake, GFF, 120, 297–306, https://doi.org/10.1080/11035899809453223, 1998.

Novak, B. and Björck, S.: A Late Pleistocene lacustrine transgression in the Fehmarn Belt, southwestern Baltic Sea, Int. J. Earth Sci., 93, 634–644, https://doi.org/10.1007/s00531-004-0429-0, 2004.

Regnéll, C., Greenwood, S. L., Gyllencreutz, R., Peterson, G., Regnéll, J., Öhrling, C., Hardeng, J., Johnson, E., Bakke, J., and Cederström, J. M.: Anchoring the Swedish Time Scale to the radiocarbon time scale – An absolute age for De Geer's zero varve, Geology, 53, 601–606, https://doi.org/10.1130/G53280.1, 2025.

Reimer, P. J., Austin, W. E. N., Bard, E., Bayliss, A., Blackwell, P. G., Ramsey, C. B., Butzin, M., Cheng, H., Edwards, R. L., Friedrich, M., Grootes, P. M., Guilderson, T. P., Hajdas, I., Heaton, T. J., Hogg, A. G., Hughen, K. A., Kromer, B., Manning, S. W., Muscheler, R., Palmer, J. G., Pearson, C., Plicht, J. v. d., Reimer, R. W., Richards, D. A., Scott, E. M., Southon, J. R., Turney, C. S. M., Wacker, L., Adolphi, F., Büntgen, U., Capano, M., Fahrni, S. M., Fogtmann-Schulz, A., Friedrich, R., Köhler, P., Kudsk, S., Miyake, F., Olsen, J., Reinig, F., Sakamoto, M., Sookdeo, A., and Talamo, S.: The IntCal20 Northern Hemisphere Radiocarbon Age Calibration Curve (0–55 cal kBP), Radiocarbon, 62, 725–757, https://doi.org/10.1017/RDC.2020.41, 2020.

Rosentau, A., Bennike, O., Uścinowicz, S., and Miotk-Szpiganowicz, G.: The Baltic sea basin, in: Submerged Landscapes of the European Continental Shelf, pp. 103–133, John Wiley & Sons, Ltd, Oxford, UK, ISBN 978-1-118-92782-3, https://doi.org/10.1002/9781118927823.ch5, 2017.

Schulze, I., Gogina, M., Schönke, M., Zettler, M. L., and Feldens, P.: Seasonal change of multifrequency backscatter in three Baltic Sea habitats, Front. Remote Sens., 3, https://doi.org/10.3389/frsen.2022.956994, 2022.

Schwarzer, K., Diesing, M., and Trieschmann, B.: Nearshore facies of the southern shore of the Baltic Ice Lake – Example from Tromper Wiek (Rügen Island), Baltica, 13, 69–76, 2000.

Stattegger, K. and Leszczyńska, K.: Rapid sea-level rise during the first phase of the Littorina transgression in the western Baltic Sea, Oceanologia, 65, 202–210, https://doi.org/10.1016/j.oceano.2022.05.001, 2023.

Svensson, N.-O.: Late weichselian and early holocene shore displacement in the central Baltic sea, Quat. Int., 9, 7–26, https://doi.org/10.1016/1040-6182(91)90059-w, 1991.

Sviridov, N. I. and Emelyanov, E. M.: Lithofacial complexes of quaternary deposits in the central and southeastern baltic sea, Lithol. Miner. Resour., 35, 211–231, https://doi.org/10.1007/BF02821956, 2000.

Talling, P. J.: How and where do incised valleys form if sea level remains above the shelf edge?, Geology, 26, 87–90, 1998.

Tauber, F.: Search for palaeo-landscapes in the southwestern Baltic Sea with sidescan sonar, Ber. RGK, 92, 323–349, 2011.

Tauber, F.: Meeresbodensedimente und Meeresbodenrelief in der deutschen Ostsee : Datenpositionen und Blattschnitt, Karte Nr. 2930 = Seabed sediments and seabed relief in the German Baltic Sea: Data positions and sheet index, map no. 2930 [Map] 1:550 000, 54° N, Hamburg, 2012.

Uścinowicz, S.: Relative Sea Level Changes, Glacio-Isostatic Rebound and Shoreline Displacement in the Southern Baltic, Polish Geological Institute Special Papers, 10, 2003.

Uścinowicz, S.: A relative sea-level curve for the Polish Southern Baltic Sea, Quat. Int., 145–146, 86–105, https://doi.org/10.1016/j.quaint.2005.07.007, 2006.

Virtasalo, J. J., Endler, M., Moros, M., Jokinen, S. A., Hämäläinen, J., and Kotilainen, A. T.: Base of brackish-water mud as key regional stratigraphic marker of mid-Holocene marine flooding of the Baltic Sea Basin, Geo-Mar. Lett., 36, 445–456, https://doi.org/10.1007/s00367-016-0464-4, 2016.

Wiberg-Larsen, P., Bennike, O., Jensen, J. B., and Lemke, W.: Trichoptera remains from early Holocene river deposits in the Great Belt, Denmark, Boreas, 30, 299–306, 2001.

Winn, K., Averdieck, F.-R., and Werner, F.: Spät- und postglaziale Entwicklung des Vejsnaes-Gebietes (Westliche Ostsee), Meyniana, 34, 1–28, 1982.

Zhurbas, V., Väli, G., Golenko, M., and Paka, V.: Variability of bottom friction velocity along the inflow water pathway in the Baltic Sea, J. Mar. Syst., 184, 50–58, https://doi.org/10.1016/j.jmarsys.2018.04.008, 2018.

Zolitschka, B., Francus, P., Ojala, A. E. K., and Schimmelmann, A.: Varves in lake sediments – a review, Quaternary Sci. Rev., 117, 1–41, https://doi.org/10.1016/j.quascirev.2015.03.019, 2015.